Poly(*N*-Vinylpyrrolidone) based biomimetic hydrogels

by
Celeste Wilken

Thesis presented in partial fulfilment of the requirements for the degree Masters of Science (Polymer Chemistry) at the University of Stellenbosch

Supervisor: Prof. Bert Klumperman
Co-supervisor: Dr. Gwen Lana-Pound
Faculty of Science
Department of Chemistry and Polymer Science

March 2012

Declaration

By submitting this thesis/dissertation electronically, I declare that the entirety of the work contained therein is my own, original work, that I am the sole author thereof (save to the extent explicitly otherwise stated), that reproduction and publication thereof by Stellenbosch University will not infringe any third party rights and that I have not previously in its entirety or in part submitted it for obtaining any qualification.

Celeste Wilken March 2012

Abstract

In the modern, fast moving society of today, there is a strong focus in research placed on the elimination of lengthy invasive medical procedures. Target specific, and chemo selective treatments are of great interest. Various advantages of this include patient comfort and over and above all cost reduction of invasive procedures. This project focused on the development of an injectable gel system with the use of biocompatible polymers. A system is regarded as injectable if the functional polymers are in solution before administration, but gels when added together. In order to design this system, one has to make use of polymers with complimentary functional groups.

Telechelic amino-functionalized PVP with narrow molecular weight distribution was synthesized via RAFT-mediated polymerization. The polymer was thoroughly characterized and cross-linked with Poly(styrene-alt-maleic anhydride) to form a three dimensional polymeric network capable of absorbing and retaining large amounts of water and or biological fluid. Unfortunately the cross-linking needed to be performed in non-aqueous solution due to hydrolysis of maleic anhydride as a competing reaction in water.

The gel was used in two model studies. The first model study focused on the attachment of a synthetic polypeptide onto the gel. The second model study evaluated the cytotoxicity effects of these gels when placed in direct contact with rodent cardiac myoblast and myocyte cells. These studies rendered promising results for future biological applications.

Opsomming

In die moderne, vinnig bewegende samelewing van vandag, word daar in navorsing, 'n sterk fokus geplaas op die uitskakeling van lang indringende mediese prosedures. Doel spesifieke, en chemo selektiewe behandelings is van groot belang. Verskeie voordele van hierdie is die toename in gemak van die pasiënt en die verlaging van kostes verbonde aan hierdie indringende prosedures. Hierdie projek het gefokus op die ontwikkeling van 'n inspuitbare gel stelsel deur gebruik te maak van biologiese aanvaarbare polimere. ‘N stelsel word beskou as inspuitbaar, indien die funksionele polimere in oplossing is voor toediening, maar wel kan gel wanneer bymekaar gevoeg word. Om hierdie tipe stelsel te kan ontwerp moet daar gebruik gemaak word van polimere met beskikbare funksionele groepe.

Telecheliese amino-funksionele Poly(*N*-vinielpirollideen) met 'n smal molekulêre gewig verspreiding is gesintetiseer deur middel van RAFT-bemiddelde polimerisasie. Die polimeer is deeglik gekarakteriseer en daarna gekruis-koppel met P(STY-*alt*-MAnh) om 'n drie-dimensionele polimeriese netwerk te vorm. Hierdie netwerk is dan ook in staat om groot hoeveelhede water en/of biologiese vloeistof te absorbeer en te behou. Ongelukkig was hierdie reaksie uitgevoer in ’n nie-waterige oplossing as gevolg van die hidrolise van Maleïne anhydride as 'n mededingende reaksie in water.

Die gel is in twee model studies gebruik. Die eerste model-studie het gefokus op die beslaglegging van 'n sintetiese polipeptied op die gel. Die tweede model studie het die sitotoksiese uitwerking van hierdie gels in direkte kontak met knaagdier hart myoblast en lymfocyten selle geëvalueer. Hierdie studies het dan ook belowende resultate vir toekomstige biologiese toepassings gelewer.

Acknowledgements

A special thanks has to go out to Prof. Klumperman for giving me this opportunity as well as granting me so much research freedom.

To Dr. Eric von Dungen, none of this would have been possible without you. Thank you for all your time, effort and patience.

Dr. Ben Loos and Delita Otto, for the entire cell work section, and putting up with my limited knowledge in this field!

Nathalie, Jaco and Gwen, thank you for all the help and explanations when I got stuck. Especially to Jaco and Nathalie for running all my GPC samples.

Elsa Malherbe for all the NMR samples!

All the staff in the polymer building that makes sure things runs smoothly: Deon, Erina, Anelie, Kelvin and Jim.

The research group, past and present, thank you for all the smiles and chats throughout the two years. It will be greatly missed!

On a more personal note: God for grating me the opportunity and being there every step of the way. To Heino, Mia, Hennie and Aimee for putting up with me daily: Anelle and Estie for being my family, I could not ask for better friends! Danie, for loving me and encouraging me to be the best that I can be. Last but not least, Dad, a simple thank you will never be enough!

Table of contents

List of Figures

List of tables

List of Schemes

List of Symbols

$M_{n(Theoretical)}$ – *Molar mass targeted when performing the polymerization*

[M]o – Initial monomer concentration

[CTA] – Initial concentration of the CTA

α – *Monomer conversion*

$M_{w(Monomer)}$ – *Molar mass of monomer*

$M_{w(CTA)}$ – *Molar mass of CTA*

$Đ$ – *Dispersity*

% S – % Swelling

M_t – *Mass of the swollen gel at time t*

M_o – *Mass of the gel at time 0*

M_s – *Mass of swollen gel at equilibrium*

M_o – *Mass of the gel at time 0*

$M_{n\ (Experimental)}$ – *Molar mass expected from* ^1H *NMR spectroscopy*

List of Abbreviations

3D – Three dimensional

UV radiation – Ultraviolet radiation

Mw – Molecular weight

PVP – Poly(N-vinyl pyrrolidone)

NVP – N-vinyl pyrrolidone

WWII – World War II

FRP – Free radical polymerization

LRP – Living radical polymerization

ATRP – Atom Transfer Radical Polymerization

NMP – Nitroxide-Mediated Polymerization

RAFT – Reversible Addition-Fragmentation chain Transfer

CSIRO – Commonwealth Scientific and Industrial Research Organization

MADIX – Macromolecular design by the interchange of xanthates

CTA – chain transfer agents

^{1}H and/or ^{13}C NMR – Proton and/or Carbon Nuclear magnetic resonance

MALDI-ToF-MS – Matrix assisted laser desorption time of flight mass spectrometry

UV-vis – Ultraviolet-Visible Spectroscopy

ATR-FTIR – Attenuated total reflectance Fourier transform infrared spectroscopy

SEC – Size exclusion chromatography

STY – Styrene

MAnh – maleic anhydride

P(STY-alt-MAnh) – poly(styrene-alt-maleic anhydride)

PEG – polyethylene glycol

THF – tetrahydrofuran

DCM – dichloromethane

DMF – N,N-dimethylformamide

AIBN – 2,2-Azobis(isobutronitrle)

PBS – Phosphate buffered saline tablets

ppm – parts per million

TMS – tetramethylsilane

HPLC grade – High Pressure Liquid Chromatography grade

DMAc – N-N-dimethylacetamide

BHT – 2,6-di-tert-butyl-4-methylphenol

LiCl – lithium chloride

PMMA – poly(methyl methacrylate)

DCTB – trans-2-[3-(4-tert-butylphenyl)-2-methyl-2-propenylidene]malononitrile

KTFA – Potassium triflouroacetic acid

HCl – Hydrochloric acid

DCC – N,N'-dicyclohexyl-carbodiimide

NHS – N-hydroxysuccinimide

MWCO – Molecular Weight Cut Off

PVP(NH_2)$_2$ – Aminolyzed PVP

P[(PEG-STY)-alt-MAnh] – polyethylene-styrene-alt-maleic anhydride

Swt % – Solid weight %

M_n – Molar mass

EWC % – Equilibrium Water Content

PI – Propidium iodide

RGD – arginine-glycine-aspartic acid

PBG – poly(benzyl-glutamate)

Dedicated to my father

"My father gave me the greatest gift anyone could give another person: he believed in me"

Jim Valvano

Chapter 1

1.1) Introduction

A hydrogel is described as a polymeric network, capable of absorbing as well as retaining a large quantity of water or biological fluids while maintaining its three-dimensional polymeric network.[1-3] The polymeric network consists of various hydrophilic areas that are hydrated in an aqueous environment resulting in the hydrogel structure. The retractive force of the three dimensional network together with the thermodynamic force of hydration will determine the amount of water at the equilibrium swollen state.[3,4] As a result of its water retaining ability and biomimetic properties, hydrogels have many uses, many of which are applicable to the biomedical field.[5]

More than any other biomaterial, hydrogels mimic natural living tissue as a result of the high water content and soft consistency.[6] The soft smooth surface of these gels further limits irritation to the surrounding tissue adding to the list of possible applications.[7]

Over the last few years much attention has been paid to *in situ* chemical polymerization.[2,5,8-12] The polymers can flow in the aqueous phase, but once injected, readily form a gel at selected conditions.[5] *In situ* synthesis of hydrogels can be divided into two major groups, namely those that form spontaneously after a trigger has been set off (*i.e.* temperature, pH, etc.) and those that are formed by UV or visible light irradiation.[11,13] Injectable systems have several advantages which include patient comfort and reduction in operational cost of the invasive procedures.[1,8]

The injectable matrix can be employed as a drug delivery vehicle[14] or as bioactive molecules that can be incorporated into the matrix before application.[15] Furthermore, thermo-sensitive hydrogels have drawn attention due to their ability to spontaneously gel at physiological temperatures.[5,16]

The challenge lies in designing a system that has enough active sites for attachment of proteins, growth factors and/or drug molecules, which will gel upon administration and remain stable for targeted or unlimited periods depending on the application. Furthermore the gel has to be able to absorb and retain enough biological fluid in order to mimic the consistency of normal living cells. But above all, the gel has to be biocompatible and not result in adverse side reactions when injected into the body.

1.2) Aim of this study

The aim of this study was to develop an injectable gel onto which a growth factor, protein and or drug molecule can be attached, that will gel upon simple injection of the two reactive polymers into a physiological environment. These gels will be synthesized by cross-linking a telechelic functionalized polymer with a multi-functional polymer.

The requirements for the gel are as follows: (1) Gelation must be able to take place in an aqueous medium at 37 °C within the pH range of 6-8. (2) Gelation must take place quickly without the release of toxic by-products so that the gel is biocompatible. (3) The reaction must be highly selective and target specific.[2] (4) Cross linking kinetics of the polymers have to be slower than the diffusion rate in order for the polymers to mix properly, but fast enough to give a gel within a few minutes.[17]

1.3) General outline of the thesis

The general outline of the thesis is as follows. *Chapter 2* describes a general historic outline and literature review regarding gels and chemistry behind it. *Chapter 2* furthermore discusses the polymers of choice and the methods employed to synthesize and characterize these polymers.

Chapter 3 contains all the experimental methods, materials and conditions, in addition to a description of the instrumentation used for characterization of the polymers and hydrogels.

In *Chapter 4*, focus is placed on characterization of the polymers synthesized in *Chapter 3*. Additionally, gel formation is discussed here as well as characterization and swelling studies done on the gels.

Chapter 5 is dedicated to two model studies performed on the gels. The first model study looked at the attachment/interaction of a synthetic peptide to/with the gel. The second model study investigates the effect that the gels, synthesized in *Chapter 3*, have on cardiac myoblast rodent cells when placed in direct contact with the cells. Morphological changes of the cells were monitored and cell death was quantified by means of fluorescence microscopy studies.

Chapter 6 provides an overview of the conclusions derived from this work, in addition to trials and tribulations encountered during the course of this study. *Chapter 6* also discusses the future outlook of the study, and provides recommendations

References

(1) Scales, C. W.; Convertine, A. J.; McCormick, C. L. *Biomacromolecules* **2006**, *7*, 1389.

(2) Ossipov, D. A.; Brannvall, K.; Forsberg-Nilsson, K.; Hilborn, J. *J. Appl. Polym. Sci.* **2007**, *106*, 60.

(3) Kopecek, J.; Yang, J. *Polym. Int.* **2007**, *56*, 1078.

(4) Kaneko, D.; Gong, J. P.; Osada, Y. *J. Mater. Chem.* **2002**, *12*, 2169.

(5) Yu, L.; Ding, J. *Chem. Soc. Rev.* **2008**, *37*, 1473.

(6) Devine, D. M.; Devery, S. M.; Lyons, J. G.; Geever, L. M.; Kennedy, J. E.; Higginbotham, C. L. *Int. J. Pharm.* **2006**, *326*, 50.

(7) Hennink, W. E.; van Nostrum, C. F. *Adv. Drug Delivery Rev.* **2002**, *54*, 13.

(8) Balakrishnan, B.; Jayakrishnan, A. *Biomaterials* **2005**, *26*, 3941.

(9) Jin, R.; Moreira Teixeira, L. S.; Krouwels, A.; Dijkstra, P. J.; van Blitterswijk, C. A.; Karperien, M.; Feijen, J. *Acta Biomater.* **2009**, *6*, 1968.

(10) Chitkara, D.; Shikanov, A.; Kumar, N.; Domb, A. J. *Macromol. Biosci.* **2006**, *6*, 977.

(11) Van Tomme, S. R.; Storm, G.; Hennink, W. E. *Int. J. Pharm.* **2008**, *355*, 1.

(12) Ossipov, D. A.; Piskounova, S.; Hilborn, J. *Macromolecules* **2008**, *41*, 3971.

(13) Jin, R.; Hiemstra, C.; Zhong, Z.; Feijen, J. *Biomaterials* **2007**, *28*, 2791.

(14) Phillips, M. A.; Gran, M. L.; Peppas, N. A. *Nano Today* **2010**, *5*, 143.

(15) Tabata, Y.; Hijikata, S.; Ikada, Y. *J. Controlled Release* **1994**, *31*, 189.

(16) Boesel, L. F.; Reis, R. L.; Roman, J. S. *Biomacromolecules* **2009**, *10*, 465.

(17) Ossipov, D. A.; Hilborn, J. *Proceeding of the 8th Polymers for Advanced Technologies International Symposium* **2005**.

Chapter 2

2.1) Introduction into hydrogels

2.1.1) History

A **gel** is a solid, jelly-like material that exhibits little to no flow when in the steady-state. Gels consist mostly of liquid, yet they behave like solids due to a three-dimensional cross-linked network within the liquid. Various types of gels are known, amongst which are xerogels and hydrogels. **Hydrogels** are super absorbent gels capable of retaining large amounts of aqueous liquid.

The history of this field dates back to 1954 when Wichterle *et al.* developed a hydrogel consisting of a copolymer of 2-hydroxyethyl methacrylate and ethylene dimethacrylate. However, it was only in 1961 that this material was applied for use in contact lenses.[1] Since then hydrogels have found wide spread applications as functional materials in diapers, breast implants, soft medicinal capsules, catheter lines, and topical creams. A few examples of natural hydrogels are found in the human body and include cartilage, mucus, and the vitreous humor of the eyes of vertebras.[2-12]

2.1.2) What is a hydrogel?

Hydrogels can be composed of natural and/or synthetic polymers and are generally described as a structure consisting of a three-dimensional polymeric network.[13] A unique property of hydrogels is their ability to absorb and retain large quantities of water or biological fluids without significant alterations to their 3D polymeric structure.[10,14,15] Gels have the ability to undergo major deformation as a result of the soft and wet surface.[16]

2.1.3) Uses of hydrogels

Hydrogels composed of biocompatible synthetic polymers are frequently used in biomedical and pharmaceutical fields. Applications include electrode sensors, articular cartilage, contact lenses, plasma expander, tissue scaffolds, matrices for cell encapsulation, artificial corneas, catheters and drug delivery vehicles.[4,12,17,18]

In recent years much of the research in the biomedical field has focused on minimizing invasive medical procedures and target specific drug delivery, which offer various advantages, such as cost reduction and patient comfort. This prompted research into injectable systems that can be administered into a specific area of the human body.[19] Possible applications include target specific drug delivery and temporary scaffolds for tissue engineering.[20] Tissue engineering specifically looks at restoring and/or repairing of damaged tissue, making site-specific administration of utmost importance. This makes injectable systems an appealing method of administration.

As mentioned before, biocompatible hydrogels have many advantages and consequently, biocompatible hydrogels are being investigated as injectable systems. A gel is regarded as injectable if the compounds are in solution before gelation and the sol-gel transition takes place rapidly upon injection.[11] There are many examples in literature in which *in situ* gelation of the gels was achieved either by means of UV-radiation or by reaction of complimentary chemical groups.[1,15]

2.1.4) What are biocompatible hydrogels?

Biocompatibility of synthetic hydrogels, with prospective medical applications, is a major field of research. When a foreign 'object' is implanted into the body, the body begins its natural healing process *i.e.* inflammation, wound healing and foreign body reaction. The processes after the implantation or application of the hydrogel are thus dependent on the physical and chemical structure of the hydrogel as well as the surface configuration.[10] An object is referred to as biocompatible when the body has no adverse side reactions due to its presence.

More than any other biomaterial, hydrogels mimic natural living tissue as a result of the high water content and soft consistency.[8] The soft and smooth surface of these gels further limits irritation to the surrounding tissue thereby increasing the list of possible applications.[21] The porosity of the hydrogels allows for the transport of low molecular weight compounds through the hydrogel.[4] Owing to the physical properties of hydrogels, they exhibit a low interfacial tension with the surrounding tissue *i.e.* the adhesive forces between the hydrogel and the surrounding tissue are very low. This results in minimal interaction between the hydrogel and surrounding tissue, which limits any biological rejection mechanism. The synthesis of a material that is 100 % biocompatible proves to be a continuous challenge for scientists.[4]

In most medical applications, the biodegradability of the hydrogels is of utmost importance. For instance, when the hydrogel is used as a matrix for drug delivery, the hydrogel needs to degrade in order for the drug to be released, so that it can be taken up by the body. To assist in this process,

labile bonds that can be broken by physiological reactions, enzymes and/or chemical reactions are often introduced into these hydrogel networks. These bonds can be found in the polymer backbone or in the cross-links that are used to prepare the gels. Knowledge of the degradation kinetics and factors affecting these would prove to be advantageous. The degradation products have to be of low toxicity and excretion has to be possible via renal clearance (M_W < 30 000g/mol).[21] The contrary is true for gels that are used as implants or other more permanent applications where the stability and non-degradability are important properties for these systems.[7] When used as a scaffold for tissue engineering or as implants, the gel should not degrade, and care has to be taken to understand the relationship between the degree of swelling due to fluid retention and the covalent bonds that have formed as part of the cross-linked polymer network.[7]

2.2) Gel chemistry

Gels seem like ideal materials with endless applications, but the question comes to mind, how do these structures maintain their 3D network? This is as a result of cross-linking of the polymer chains shown in *Figure 2.1*. Cross-links are present in these networks to avoid the dissolution of the hydrophilic polymer chains/segments into the solvent. The degree of cross-linking greatly affects the *in vivo* performance, the porosity of the gel, the degree of swelling and the sorption kinetics. These physical properties of the gel greatly affect the end application.[4,21-23]

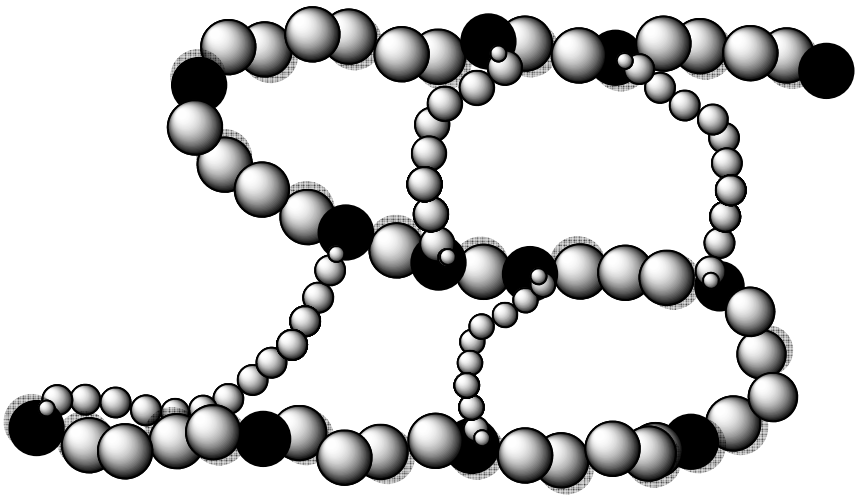

Figure 2.1: Cross-linked polymer network.

Cross-links can either be physical or chemical and as a result, there is a wide variety of methods for the preparation of gels with different structures and properties.[10]

Chemical cross-linking reactions include photo-cross-linking reactions, Michael-type reactions and Schiff base formation reactions, to name but a few. Dissolution of these chemically cross-linked segments is prevented by the covalent bonds that are formed between the reactive groups on the separate chains. Physical cross-linking methods include hydrophobic interactions, ionic interactions and stereo-complexation, with dissolution being prevented by the physical interaction between the different polymer chains.[24]

Chemically cross-linked hydrogels are chemically and mechanically more stable than physically cross-linked gels, but this often results in toxic byproducts and/or requires organic solvents for their preparation. Covalently bonded gels can be obtained by cross-linking of reactive polymer precursors with a low M_w cross-linking agent, cross-linking through polymer-polymer reactions as well as cross-linking during copolymerization.[10]

Ultimately, the end-application will determine the type of cross-linking system that will be used. The higher the degree of cross-linking, the stronger the gel, but the more brittle and less porous the structure of the hydrogel.[25] Therefore it is important to establish the optimum degree of cross-linking in order to obtain a strong yet elastic gel.

There are a few approaches to the synthesis of gels. One approach involves mixing two polymer components each, with their own type of complementary functionality, capable of reacting chemo-selectively and quickly under physiological conditions.[26] Electrostatic, hydrophobic and end-group specific interactions can also be used to design *in situ* gelation systems.[14]

In situ gels can be divided into two major groups namely those that form spontaneously after a trigger has been set off (*i.e.* temperature, pH, etc.) and those that are formed by UV or visible light irradiation.[1] Although much attention has been given to photo-polymerizable gels in literature, in the context of this project the main focus will be on instant gels that form without the application of an external trigger.

Copolymerization of a cross-linking agent with a monomer of choice is a common method of synthesizing gels.[10] An alternative involves the synthesis of interpenetrating networks, *i.e.* a system consisting of two separately cross-linked networks that are inter-twined.

The cross-linking of a reactive polymer with a low molecular weight agent containing complementary reactive functional groups could be used to obtain a gel.[10] Covalent bonds between

the polymer chains can be achieved by the chemical reaction of the complimentary functional groups. The functional groups must be able to react chemo-selectively under physiological conditions. These reactions include addition and condensation reactions. However one needs to bear in mind that all products formed have to be non-toxic for the purpose of biomedical applications.

More specific to this project, by reacting an α,ω-telechelic with the functional groups of a multi-functional polymer, gels can be obtained through addition reactions.[21]

2.3) Polymer used in this study

The polymer(s) of choice when designing biocompatible systems need(s) careful consideration. Specifically for biomedical applications, the polymers and other compounds used have to be non-toxic and preferably degradable without the release of toxic byproducts. Poly(*N*-vinyl pyrrolidone) (PVP) (*Scheme 2.1*) is one such non-toxic polymer, albeit non-degradable.

PVP was first synthesized from the monomer *N*-vinyl pyrrolidone (NVP) by Reppe *et al.* and has since been used in various biomedical applications.[27]

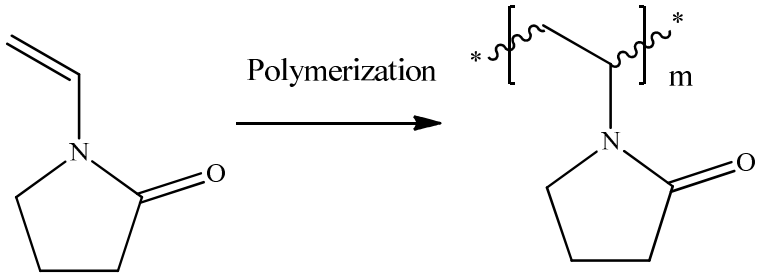

Scheme 2.1: Monomer NVP to polymer PVP.

During WWII, PVP was used as a blood plasma expander and currently it is a major component of certain contact lenses.[28,29] Medically, PVP is restricted to products that are taken in orally or topically, as it was found that PVP cannot be broken down sufficiently in the body.[30,31] PVP has also been used in conjugation with proteins, peptides and drug molecules as it is said to reduce toxicity and increase solubility of these compounds.[32,33,34]

PVP is also found in various cosmetics, shaving products, and hair styling products. Its widespread use has been extensively reviewed.[12,35-38]

In order to limit toxicity it is necessary to eliminate the use of organic solvents. PVP in this sense is ideal since it is soluble in water as well as in most organic solvents.[39] PVP is a highly hydrophilic, stable, biocompatible polymer with unique complexing abilities.[12] Furthermore, its unique chelating ability accounts for the use of this polymer in food and drug delivery as a chelating agent.[35] These advantages make PVP a suitable candidate when designing a biomimetic hydrogel. PVP has been functionalized in various ways to serve as a cross-linker and its cross-linking ability has been well documented in literature.[27] Another challenge lies in choosing another biocompatible polymer with complimentary functional groups for reaction with chain end functionalized PVP.

2.3.1) Synthesis of PVP via RAFT-mediated polymerization

Free radical polymerization (FRP) is one of the most versatile methods of polymerization, usually making use of initiators such as azo or peroxide compounds. The first step in this polymerization process is initiation, followed by the propagation step. The chain then grows by addition of monomer to the growing radicals that were formed. Termination of the growing chain takes place by either radical coupling or by disproportionation between radicals as seen in *Scheme 2.2*.[27] FRP processes are used by many research laboratories owing to their tolerance against water, the presence of small amounts of oxygen and a wide variety of functional groups.

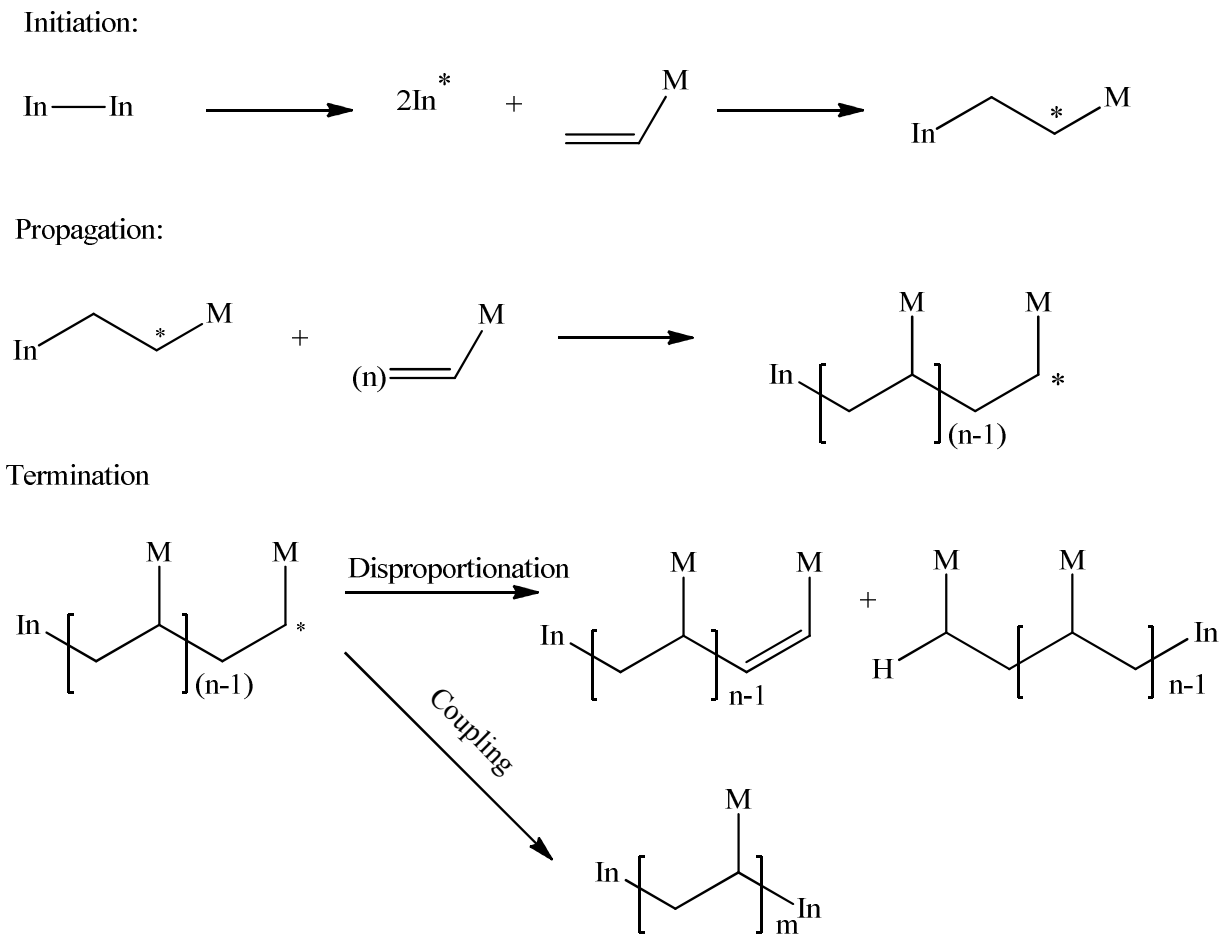

Scheme 2.2: Mechanism for free radical polymerization.

A major drawback of free radical polymerization is poor control over molar mass distribution. This is partially caused by the occurrence of chain transfer reactions to monomer and/or solvent. These chain transfer reactions further result in poor control over chain-end functionality, posing various problems when it comes to post polymerization functionalization.[23]

Controlled or living radical polymerization (LRP) is a type of radical polymerization where the majority of polymer chains are in a dormant state. LRP is unique in the sense that only a small fraction of the chains undergo irreversible termination. This results in polymer chains with a narrow molar mass distribution and a predetermined molar mass as a result of the chains growing simultaneously throughout the polymerization. It further allows control over the chain-end functionalities. The lifetime of the growing polymers is increased by introducing the dormant state for the active/growing polymer chains, resulting in chains growing at the same rate. This process continues until all monomer has been used up. With NVP polymerization, care has to be taken to

ensure that the reaction is stopped at low conversions in order to ensure chain-end functionalities are preserved.

Various techniques have been proposed for the controlled polymerization of NVP, such as Atom Transfer Radical Polymerization (ATRP), Nitroxide-Mediated Polymerization (NMP), Organostibine mediated LRP, Organotellerium mediated LRP and Reversible Addition-Fragmentation chain Transfer (RAFT) mediated polymerization.[40-43]

Until recent years, the polymerization of NVP was only reported via conventional radical polymerization. Neither NMP nor ATRP has been successfully used for the synthesis of PVP with a narrow molar mass distribution.[44] For this reason these techniques are not discussed in this text. The introduction of RAFT-mediated polymerization (*Scheme 2.3*) by Chiefari *et al.*[45] resulted in the controlled polymerization of a wider range of functional monomers, including NVP, in various organic and aqueous media.[44,46] RAFT-mediated polymerization allows for the production of polymers under a wide range of conditions and provides controlled molecular weight polymers with narrow molar mass distribution and allows for the preparation of block copolymers.[45,47,23] Additionally it allows for the introduction of a wide range of functionalities at the α and ω-chain ends of the polymer.[44,45,48-51] RAFT-mediated polymerization is flexible in the sense that it not only allows the synthesis of polymers with chain-end functionalities, but also allows for post-polymerization modification of these polymers due to the retention of chain-end functionalities after polymerization.[44,49-59] Post-polymerization reactions, such as hydrolysis, aminolysis and thermolysis can be used to introduce thiol, hydroxyl, primary amine and aldehyde functionalities.[52,54,60-62]

RAFT or Macromolecular design by the interchange of xanthates (MADIX) as published by CSIRO[45] (Commonwealth Scientific and Industrial Research Organization) and Rhodia research group[63] respectively, reported the use of chain transfer agents (CTAs) that consisted of a thiocarbonyl-thio moiety. Zard *et al.* specifically made use of xanthates as CTAs.[63,64]

Initiation and Propagation:

Addition to the RAFT agent:

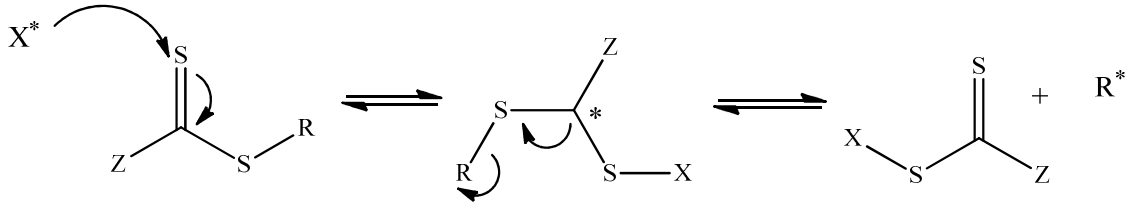

Reinitiation:

Equilibrium conditions of RAFT mediated polymerization:

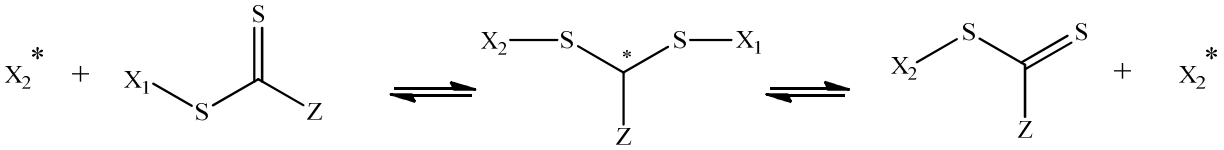

Termination:

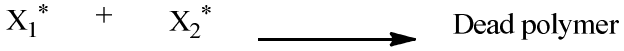

Scheme 2.3: Generally accepted RAFT mechanism.

The choice of RAFT agent needs careful consideration. A high chain transfer constant results in fast interchange between active and dormant chains. The concentration of radicals (active chains) is controlled by initiation/termination (like in FRP). Moad *et al.* published clear considerations that need to be taken into account when choosing the RAFT agent.[50] Firstly, the C=S bond of the RAFT agent needs to have a high addition rate constant. Secondly, the intermediate radicals have to fragment easily to render the active species. Lastly, the leaving group radicals formed after fragmentation should be able to reinitiate the polymerization rapidly and efficiently.

The two functional groups of the RAFT agent are the R-group and the Z-group. The R-group is referred to as the leaving group and the Z-group referred to as the activating group.[65]

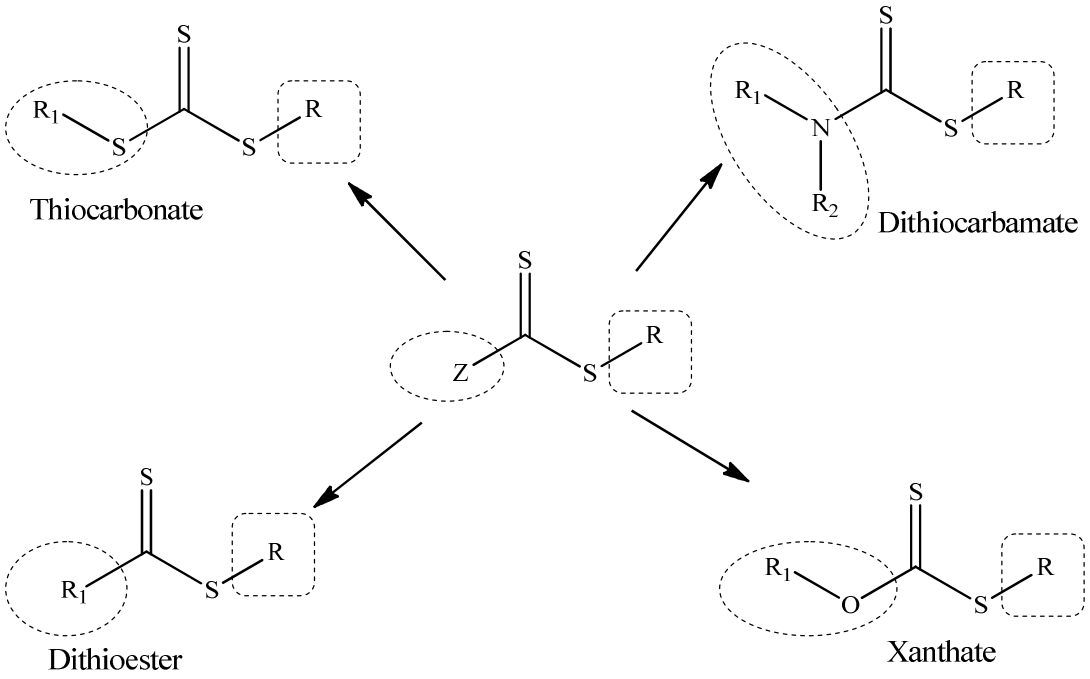

Figure 2.3: Commonly used RAFT agents.

The RAFT process involves insertion of monomer between the sulfur of the thiocarbonyl-thio group and the R-group.[66] The R-group needs to be a good homolytic leaving group, keeping in mind the steric and electronic factors that could influence the leaving ability of the group. Furthermore, the R-group must be a good re-initiating radical for the particular monomer. This group is then also responsible for the functionality of the alpha chain-end, and can be chosen to be chemically active for post polymerization functionalization.[50]

Additionally the activating group referred to as the Z-group must be able to activate the C=S bond towards radical addition. The Z-group must stabilize the intermediate radical that forms when the propagating radical adds to the RAFT agent as well as maintain sufficiently high fragmentation rates of the intermediate radical.[45] RAFT allows for very good control over the polymerization of NVP, which is a fast propagating monomer.[47,67]

One of the main advantages of utilizing RAFT agents is that the resulting polymer chain ends can be characterized by the presence of the Z- and R-groups of the RAFT agent at the α- and ω-chain-ends of the polymer. Furthermore, the R and Z functionalities of the RAFT agent serve as a powerful tool/handle to insert or attach molecules of interest at the polymer chain

end (*Scheme 2.4*). It is important to note that the original thiocarbonyl-thio group is retained in the polymeric product and thus serves as the dormant form of the propagating radical, which provides the polymerization process with a living character. It is also due to this reason that the process is suitable to synthesize block copolymers and chain-end functionalized polymers.[66]

During the course of this project, xanthate RAFT agents were synthesized and investigated for the polymerization of NVP. The choice to make use of xanthate RAFT agents was a result of the fact that the O atom is adjacent to an electron-withdrawing group. As a result, the lone electron pair on the O atom is less available to interact with C=S double bond. This facilitates good control over the molecular weight distribution in the polymerization of poorly stabilized vinyl monomers like NVP and vinyl acetate, which are fast propagating.[44,47,67-69]

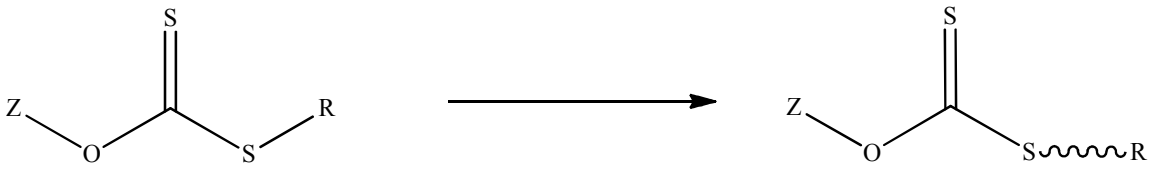

Scheme 2.4: RAFT-mediated polymerization.

In some cases, a drawback with RAFT-mediated polymerization is retardation. Various reasons have been proposed for this, including the presence of oxygen, and/or impurities in the RAFT agent itself. In the case of retardation during RAFT-mediated polymerization, the effect increases with an increase of RAFT agent concentration.[70] Although the drawback is a cause of concern, the inherent advantages of this polymerization technique outweigh the disadvantages.

2.4) Characterization of the polymers

All polymers synthesized were characterized by means of NMR spectroscopy,[47,56,67,71-73] MALDI-TOF-MS,[56,57,72-76] UV-vis spectroscopy,[29,71] ATR-FTIR spectroscopy[25,71,77-80] and SEC.[81] These techniques are discussed in detail in Chapter 3.

2.5) Toxicity

A particular area of interest is the toxicity of polymers synthesized via RAFT-mediated polymerization. The reactive thiocarbonyl-thio groups of the RAFT polymers raise the biggest concern when these polymers are synthesized for potential biological applications.[53] Several reports have documented that removal of the thiocarbonyl-thio group is possible via post polymerization treatments, although the extra reaction step and potentially unwanted side reactions should be investigated. However, in the case of PVP, the chain transfer agent (xanthate) is easily removed.[14,59,66,82]

2.5.1) Cell studies

There are various studies in literature where the effect of PVP in direct contact with cells was investigated.[5,8,12,13,28,83] Some found PVP to stimulate cell growth, whereas others found it as a cause of irritation. Chapter 5 will discuss cell studies and related issues in more detail.

2.6) Conclusions

When designing a hydrogel for biological applications, there are various factors that need careful consideration. The hydrogel has to be biologically inert with no release of toxic byproducts upon synthesis and possible degradation. Preferably, gelation has to take place under physiological conditions *i.e.* temperature and pH range of the body, as well as remain stable under these conditions.[84] Furthermore, methods should be investigated to ensure that the polymer stays in the body for the targeted period of time. The use of toxic organic solvents needs to be eliminated as far as possible. It is important to note that evaluation of the toxicity of these compounds needs to happen on a case-by-case basis and that generalization based on classes cannot be made.[53]

References

(1) Van Tomme, S. R.; Storm, G.; Hennink, W. E. *Int. J. Pharm.***2008**, *355*, 1.

(2) Zhang, Z.; Chen, L.; Deng, M.; Bai, Y.; Chen, X.; Jing, X. *J. Polym. Sci., Part A: Polym. Chem.***2011**, *49*, 2941.

(3) Zhu, J. *Biomaterials***2010**, *31*, 4639.

(4) Ratner Buddy, D.; Hoffman Allan, S. In *Hydrogels for Medical and Related Applications*; American Chemical Society:**1976**; Vol. 31, p 1.

(5) Bischoff, F. *Clin. Chem.***1972**, *18*, 869.

(6) Peppas, N. A.; Bures, P.; Leobandung, W.; Ichikawa, H. *Eur. J. Pharm. Biopharm.***2000**, *50*, 27.

(7) Hoffman, A. S. *Adv. Drug Delivery Rev.***2002**, *54*, 3.

(8) Devine, D. M.; Devery, S. M.; Lyons, J. G.; Geever, L. M.; Kennedy, J. E.; Higginbotham, C. L. *Int. J. Pharm.***2006**, *326*, 50.

(9) Gupta, K. M.; Barnes, S. R.; Tangaro, R. A.; Roberts, M. C.; Owen, D. H.; Katz, D. F.; Kiser, P. F. *J. Pharm. Sci.***2007**, *96*, 670.

(10) Kopecek, J.; Yang, J. *Polym. Int.***2007**, *56*, 1078.

(11) Yu, L.; Ding, J. *Chem. Soc. Rev.***2008**, *37*, 1473.

(12) Ma, R.; Xiong, D.; Miao, F.; Zhang, J.; Peng, Y. *Mater. Sci. Eng., C.***2009**, *29*, 1979.

(13) Benamer, S.; Mahlous, M.; Boukrif, A.; Mansouri, B.; Youcef, S. L. *Nucl. Instrum. Methods Phys. Res., Sect. B.***2006**, *248*, 284.

(14) Scales, C. W.; Convertine, A. J.; McCormick, C. L. *Biomacromolecules.***2006**, *7*, 1389.

(15) Ossipov, D. A.; Brannvall, K.; Forsberg-Nilsson, K.; Hilborn, J. *J. Appl. Polym. Sci.***2007**, *106*, 60.

(16) Kaneko, D.; Gong, J. P.; Osada, Y. *J. Mater. Chem.***2002**, *12*, 2169.

(17) Lee, S. G.; Brunello, G. F.; Jang, S. S.; Lee, J. H.; Bucknall, D. G. *J. Phys. Chem. B.***2009**, *113*, 6604.

(18) Kim, J. S.; Park, J. S.; Kim, S. I. *React. Funct. Polym.***2003**, *55*, 53.

(19) Chitkara, D.; Shikanov, A.; Kumar, N.; Domb, A. J. *Macromol. Biosci.***2006**, *6*, 977.

(20) Boesel, L. F.; Reis, R. L.; Roman, J. S. *Biomacromolecules.***2009**, *10*, 465.

(21) Hennink, W. E.; van Nostrum, C. F. *Adv. Drug Delivery Rev.***2002**, *54*, 13.

(22) Khurma, J. R.; Rohindra, D. R.; Nand, A. V. *Polym. Bull. (Berlin.)***2005**, *54*, 195.

(23) Eksteen, Z., MSc thesis, University of Stellenbosch, South Africa, 2009.

(24) Jin, R.; Hiemstra, C.; Zhong, Z.; Feijen, J. *Biomaterials.***2007**, *28*, 2791.

(25) Devine, D. M.; Higginbotham, C. L. *Eur. Polym. J.***2005**, *41*, 1272.

(26) Ossipov, D. A.; Hilborn, J. *Proceeding of the 8th Polymers for Advanced Technologies International Symposium.***2005**.

(27) Pfukwa, R., MSc thesis, University of Stellenbosch, South Africa, 2008.

(28) Niu, G.; Yang, Y.; Zhang, H.; Yang, J.; Song, L.; Kashima, M.; Yang, Z.; Cao, H.; Zheng, Y.; Zhu, S.; Yang, H. *Acta Biomater.***2009**, *5*, 1056.

(29) Pound, G., PhD thesis, University of Stellenbosch, South Africa, 2008.

(30) Ranucci, E.; Macchi, L.; Annunziata, R.; Ferruti, P.; Chiellini, F. *Macromol. Biosci.***2004**, *4*, 706.

(31) Trimpin, S.; Eichhorn, P.; Rader, H. J.; Mallen, K.; Knepper, T. P. *J. Chromatogr. A.***2001**, *938*, 67.

(32) Kamada, H.; Tsutsumi, Y.; Yamamoto, Y.; Kihira, T.; Kaneda, Y.; Mu, Y.; Kodaira, H.; Tsunoda, S.; Nakagawa, S.; Mayumi, T. *Cancer Res.***2000**, *60*, 6416.

(33) D'Souza, A. J. M.; Schowen, R. L.; Topp, E. M. *J. Controlled Release.***2004**, *94*, 91.

(34) Tsunoda, S.; Kamada, H.; Yamamoto, Y.; Ishikawa, T.; Matsui, J.; Koizumi, K.; Kaneda, Y.; Tsutsumi, Y.; Ohsugi, Y.; Hirano, T.; Mayumi, T. *J. Controlled Release.***2000**, *68*, 335.

(35) Yanpeng, J.; Zonghua, L.; Shan, D.; Lihua, L.; Changren, Z. *J. Appl. Polym. Sci.***2006**, *101*, 1515.

(36) Kadlubowski, S.; Henke, A.; Ulanski, P.; Rosiak, J. M.; Bromberg, L.; Hatton, T. A. *Polymer.***2007**, *48*, 4974.

(37) Jin, S.; Liu, M.; Chen, S.; Gao, C. *Eur. Polym. J.***2008**, *44*, 2162.

(38) Bueno, V.; Cuccovia, I.; Chaimovich, H.; Catalani, L. *Colloid Polym. Sci.***2009**, *287*, 705.

(39) Perrino, M. P.; Navarro, R.; Tardajos, M. G.; Gallardo, A.; Reinecke, H. *Eur. Polym. J.***2010**, *46*, 1557.

(40) Bilalis, P.; Pitsikalis, M.; Hadjichristidis, N. *J. Polym. Sci., Part A: Polym. Chem.***2006**, *44*, 659.

(41) Coessens, V.; Pintauer, T.; Matyjaszewski, K. *Prog. Polym. Sci.***2001**, *26*, 337.

(42) Lu, X.; Gong, S.; Meng, L.; Li, C.; Yang, S.; Zhang, L. *Polymer.***2007**, *48*, 2835.

(43) Ray, B.; Kotani, M.; Yamago, S. *Macromolecules.***2006**, *39*, 5259.

(44) Devasia, R.; Bindu, R. L.; Borsali, R.; Mougin, N.; Gnanou, Y. *Macromol. Symp.***2005**, *229*, 8.

(45) Chiefari, J.; Chong, Y. K. B.; Ercole, F.; Krstina, J.; Jeffery, J.; Le, T. P. T.; Mayadunne, R. T. A.; Meijs, G. F.; Moad, C. L.; Moad, G.; Rizzardo, E.; Thang, S. H. *Macromolecules***1998**, *31*, 5559.

(46) Boyer, C.; Bulmus, V.; Liu, J.; Davis, T. P.; Stenzel, M. H.; Barner-Kowollik, C. *J. Am. Chem. Soc.***2007**, *129*, 7145.

(47) Klumperman, B.; McLeary, J. B.; van den Dungen, E. T. A.; Pound, G. *Macromol. Symp.***2007**, *248*, 141.

(48) Quemener, D.; Davis, T. P.; Barner-Kowollik, C.; Stenzel, M. H. *Chem. Commun.***2006**, 5051.

(49) Moad, G.; Rizzardo, E.; Thang, S. H. *Aust. J. Chem.***2005**, *58*, 379.

(50) Moad, G.; Rizzardo, E.; Thang, S. H. *Aust. J. Chem.***2009**, *62*, 1402.

(51) Perrier, S.; Takolpuckdee, P. *J. Polym. Sci., Part A: Polym. Chem.***2005**, *43*, 5347.

(52) Zelikin, A. N.; Such, G. K.; Postma, A.; Caruso, F. *Biomacromolecules.***2007**, *8*, 2950.

(53) Pissuwan, D.; Boyer, C.; Gunasekaran, K.; Davis, T. P.; Bulmus, V. *Biomacromolecules.***2010**, *11*, 412.

(54) Pound, G.; McKenzie, J. M.; Lange, R. F. M.; Klumperman, B. *Chem. Commun.***2008**, 3193.

(55) Barner, L.; Perrier, S. *Polymers with Well-Defined End Groups via RAFT – Synthesis, Applications and Postmodifications*; Wiley-VCH Verlag GmbH & Co. KGaA, **2008**.

(56) Lai, J. T.; Shea, R. *J. Polym. Sci., Part A: Polym. Chem.***2006**, *44*, 4298.

(57) Lima, V.; Jiang, X.; Brokken-Zijp, J.; Schoenmakers, P. J.; Klumperman, B.; Van Der Linde, R. *J. Polym. Sci., Part A: Polym. Chem.***2005**, *43*, 959.

(58) Bathfield, M.; D'Agosto, F.; Spitz, R.; Charreyre, M.; Delair, T. *J. Am. Chem. Soc.***2006**, *128*, 2546.

(59) Perrier, S.; Takolpuckdee, P.; Mars, C. A. *Macromolecules.***2005**, *38*, 6770.

(60) Tasdelen, M. A.; Kahveci, M. U.; Yagci, Y. *Prog. Polym. Sci.***2011**, *36*, 455.

(61) Boyer, C.; Granville, A.; Davis, T. P.; Bulmus, V. *J. Polym. Sci., Part A: Polym. Chem.***2009**, *47*, 3773.

(62) Luo, L.; Ranger, M.; Lessard, D. G.; Le Garrec, D.; Gori, S.; Leroux, J.-C.; Rimmer, S.; Smith, D. *Macromolecules.***2004**, *37*, 4008.

(63) Charmot, D.; Corpart, P.; Adam, H.; Zard, S. Z.; Biadatti, T.; Bouhadir, G. *Macromol. Symp.***2000**, *150*, 23.

(64) Destarac, M.; Taton, D.; Zard Samir, Z.; Saleh, T.; Six, Y. In *Advances in Controlled/Living Radical Polymerization*; American Chemical Society:**2003**; Vol. 854, p 536.

(65) Thang, S. H.; Chong, Y. K.; Mayadunne, R. T. A.; Moad, G.; Rizzardo, E. *Tetrahedron Lett.***1999**, *40*, 2435.

(66) Chong, Y. K.; Moad, G.; Rizzardo, E.; Thang, S. H. *Macromolecules.***2007**, *40*, 4446.

(67) Pound, G.; McLeary, J. B.; McKenzie, J. M.; Lange, R. F. M.; Klumperman, B. *Macromolecules.***2006**, *39*, 7796.

(68) Destarac, M.; Bzducha, W.; Taton, D.; Gauthier-Gillaizeau, I.; Zard, S. Z. *Macromol. Rapid Commun.***2002**, *23*, 1049.

(69) Postma, A.; Davis, T. P.; Li, G.; Moad, G.; O'Shea, M. S. *Macromolecules.***2006**, *39*, 5307.

(70) Plummer, R.; Goh, Y.-K.; Whittaker, A. K.; Monteiro, M. J. *Macromolecules.***2005**, *38*, 5352.

(71) Zhu, X.; Lu, P.; Chen, W.; Dong, J. *Polymer.***2010**, *51*, 3054.

(72) Raith, K.; Kühn, A. V.; Rosche, F.; Wolf, R.; Neubert, R. H. H. *Pharm. Res.***2002**, *19*, 556.

(73) Ranucci, E.; Ferruti, P.; Annunziata, R.; Gerges, I.; Spinelli, G. *Macromol. Biosci.***2006**, *6*, 216.

(74) Schriemer, D. C.; Li, L. *Anal. Chem.***1997**, *69*, 4169.

(75) Schriemer, D. C.; Li, L. *Anal. Chem.***1997**, *69*, 4176.

(76) Favier, A.; Ladaviare, C.; Charreyre, M.-T.; Pichot, C. *Macromolecules.***2004**, *37*, 2026.

(77) Maeda, H. *Adv. Drug Delivery Rev.***2002**, *6*, 181.

(78) Muta, H.; Ishida, K.; Tamaki, E.; Satoh, M. *Polymer.***2002**, *43*, 103.

(79) Park, E. S.; Kim, H. S.; Kim, M. N.; Yoon, J. S. *Eur. Polym. J.***2004**, *40*, 2819.

(80) Haddadine-Rahmoun, N.; Amrani, F.; Arrighi, V.; Cowie, J. M. G. *Eur. Polym. J.***2008**, *44*, 821.

(81) Pound, G.; Eksteen, Z.; Pfukwa, R.; McKenzie, J. M.; Lange, R. F. M.; Klumperman, B. *J. Polym. Sci., Part A: Polym. Chem.***2008**, *46*, 6575.

(82) Jia, Z.; Liu, J.; Davis, T. P.; Bulmus, V. *Polymer.***2009**, *50*, 5928.

(83) Smith, L. E.; Rimmer, S.; MacNeil, S. *Biomaterials.***2006**, *27*, 2806.

(84) Monfardini, C.; Veronese, F. M. *Bioconjugate Chem.***1998**, *9*, 418.

Chapter 3

3.1) Introduction

The aim of this chapter is to describe the synthesis and characterization of telechelic amino-functionalized poly(*N*-vinyl pyrrolidone) (PVP) with narrow molar mass distribution. These polymers will be used for the synthesis of hydrogels.

Difunctional or telechelic polymers are defined as polymer chains containing two reactive end-groups that can be used for further functionalization.[1] A telechelic polymer refers to polymer chains containing the same functionality at both ends, whereas hetero-telechelic refers to polymer chains containing different functionalities at the polymer chain-ends.[2] Polymers containing two reactive chain-end functionalities have been reported as building blocks for macromolecular structures as well as chain extension molecules and cross-linking agents. The reactive end-groups can be introduced via the initiator, the RAFT agent (as in the case with RAFT-mediated polymerization) and/or via post-polymerization reactions.[1-5]

The amino-telechelic functionalized PVP synthesized in this study was used for a cross-linking reaction in order to form a three dimensional polymeric network. Covalent bonds between the polymer chains can be achieved by reaction between complimentary functional groups.[6] The challenge was to find another biocompatible or biologically inert polymer to react with the telechelic PVP.

The ability of styrene (STY) and maleic anhydride (MAnh) to form alternating copolymers has been widely published.[6-21] Copolymers with anhydride functionalities can easily be modified via reaction of the MAnh moiety with other functionalities. These often include biomolecules such as proteins, peptides and/or chemotherapeutic drugs.[22-25] This field of research has attracted much attention over the last decade.[15] The anhydride functionality readily reacts by means of hydrolysis, esterification and amidation.[19] Hydrolysis of these anhydride functionalities results in poly-electrolytes with many interesting properties.[26] Furthermore, cross-linkers containing a hydroxyl or amino functionality readily react with poly(styrene-*alt*-maleic anhydride) (P(STY-*alt*-MAnh)) by

means of a ring-opening reaction.[13] The amino functionality of the telechelic PVP used in this study introduces reactivity towards the MAnh units present in P(STY-*alt*-MAnh).

In view of the potential biological application of the gel, it is desirable to design a system that is completely solvent free in order to limit toxicity of the system. Although the polymers of choice were carefully chosen due to their biocompatibility, the solvents used are still a cause of concern. Unless this can be completely eliminated, the system will not be able to be labelled 'biocompatible'.

Another aim in this study was to attach a polyethylene glycol (PEG) moiety to the STY unit of P(STY-*alt*-MAnh). This would then result in a water soluble system with all MAnh units intact for further reactions. PEG has been FDA approved and has since been used in many biological applications.[27] Among the various useful properties of PEG is the fact that it is soluble in many organic solvents as well as in water.[28] The attachment of PEG to insoluble compounds/polymers to improve water solubility has been widely published.[29-31] PEG is suitable for this purpose because the polymer backbone is chemically inert, although the terminal methoxy or hydroxyl group allow for chemical modification or reaction with another polymer. These properties of PEG resulted in the idea to attach a PEG chain to STY in P(STY-*alt*-MAnh) in order to make this polymer water-soluble, whilst still keeping the maleic anhydride functionalities intact. Thus the MAnh units would still be available for reaction with PVP with the advantage that the reaction would now take place in water. The grafting of PEG onto P(STY-*alt*-MAnh) via the MAnh units has been reported.[32] This was reported as a straight forward procedure. However, in this study it was not ideal as this reaction would limit the number of reactive points available for reaction with $PVP(NH_2)_2$.

In conclusion, the aim of this study was to synthesize hydrogels via reaction of telechelic amino-functionalized PVP with P(STY-*alt*-MAnh) and P(STY-*alt*-MAnh) derivatives. Hydrogels obtained in this study will be undergoing a cytotoxicity evaluation. The results of those evaluations will be discussed in Chapter 5.

3.2) Experimental details

3.2.1) Materials

Potassium-*O*-ethyl xanthate (95 %, Merck), 2-bromopropionic acid (98 %, Fluka), sodium hydroxide (Saarchem), 25 % ammonia solution (Merck), *N*-hydroxysuccinimide (98 %, Aldrich),

N,N'-dicyclohexyl-carbodiimide (99 %, Aldrich), 1,3-diaminopropane (99 %, Aldrich) and magnesium sulphate (Merck), were used as received.

1,4-dioxane, tetrahydrofuran (THF, Aldrich, 98 %), diethyl ether (KIMIX, CP-grade, 99.5 %.), chloroform (KIMIX, CP-grade, 99.5 %.) and dichloromethane (DCM, KIMIX, CP-grade, 99.5 %.) were dried over molecular sieves (4 Å, 1.6 mm pellet). 37 % Hydrochloric acid (HCl, Aldrich), ethyl acetate (KIMIX, CP-grade, 99.5 %), ethanol (KIMIX, CP-grade, 99.5 %), hexane (KIMIX, CP-grade, 99.5 %) and *N,N*-dimethylformamide (DMF, 99.8 % Sigma) were reaction grade and used without further purification.

2,2-Azobis(isobutyronitrile) (AIBN) was recrystalized twice from methanol. Phosphate buffered saline tablets (Merck) were used to make up a PBS solution. P(STY-*alt*-MAnh) (M_n: 35000 g/mol) and *p*-vinyl benzyl-poly(ethylene glycol) (M_n: 660 g/mol) were synthesized within the research group. Distillation of NVP was performed under reduced pressure (< 1 mbar) at 74 ºC.

3.2.2) Instrumentation

3.2.2.1) Nuclear magnetic resonance (NMR) spectroscopy

^{1}H NMR and ^{13}C NMR spectra were obtained in $CDCl_3$ with a Varian VXR-Unity (400 MHz) spectrometer. Chemical shifts are reported in parts per million (ppm) and tetramethylsilane (TMS) was used as internal reference.

3.2.2.2) Size exclusion chromatography (SEC)

The SEC setup consisted of a Waters Alliance apparatus, fitted with a 50x8 mm guard column in series with three 300x8 mm, 10 µm particle size GRAM columns (2 x 3000 Å and 100 Å)obtained from PSS, a Shimadzu LC-10AT isocratic pump, a Waters 171+ autosampler, a refractive index detector and a Waters 2487 dual wavelength UV detector. The flow rate was set at 1 mL/min, and the injection volume was 100 µL. The solvent used was HPLC grade, *N-N*-dimethylacetamide (DMAc), with 0.05 % w/v 2,6-di-*tert*-butyl-4-methylphenol (BHT) and 0.03 % w/v lithium chloride (LiCl). The calculated molar masses were based on a calibration curve for poly(methyl methacrylate) (PMMA) standards (molar mass range 850 to 3.5×10^5 g/mol) of low dispersity from Polymer Laboratories. Data acquisition and processing were performed with Millemium[32] software (Version 4).

3.2.2.3) Ultraviolet-Visible (UV-Vis) Spectroscopy

A Perkin Elmer Lambda 20 photodiode array spectrophotometer was used to measure the UV-Vis spectra. It consisted of a holographic monochromator, pre-aligned deuterium and halogen lamps and a photodiode array detector. UV Winlab (version 2.0) software was used for data acquisition and processing. Operating temperature was 25 ºC.

3.2.2.4) Attenuated total reflectance Fourier transform infrared spectroscopy (ATR-FTIR)

IR spectra were recorded using a Thermo-Nicolette iS10 FTIR with a ZnSe ATR attachment and an LC-transform attachment. This allowed the examination of samples in solid or liquid state without prior sample preparation. Spectra were recorded from 500 cm^{-1} to 4000 cm^{-1}.Resolution was set to 8 cm^{-1}, with 32 scans per sample. Omnic spectra software (version 8.1) was used for all data acquisition and processing.

3.2.2.5) Matrix assisted laser desorption time of flight mass spectrometry (MALDI-TOF-MS)

MALDI-TOF-MS analysis was carried out on a Voyager-DE STR form Applied Biosystems. The laser frequency was 20 Hz, 337 nm with an acceleration voltage of 25 kV. The matrix material used was trans-2-[3-(4-tert-butylphenyl)-2-methyl-2-propenylidene]malononitrile (DCTB) (40 mg/mL). The sample was dissolved in HFIP (1 mg/mL). The matrix, ionization agent and sample were mixed (5:1:5) and placed on the target plate. Potassium triflouroacetic acid (KTFA) was added as cationic ionization agent (5 mg/mL).

3.2.3) Synthetic section

The next section contains all experimental procedures and details for all experiments described in this thesis.

3.2.3.1) Chain transfer agents

3.2.3.1.1) Synthesis of xanthate chain transfer agent (CTA)(Compound A)

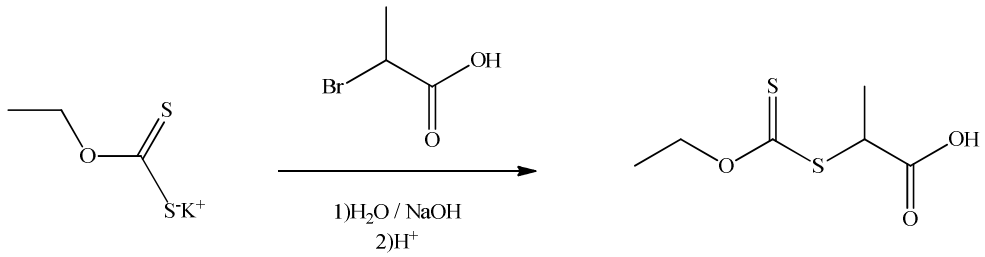

Scheme 3.1: Synthetic route for compound A.

30 g distilled water was used to dissolve potassium-*O*-ethyl xanthate (10.08 g, 6.25×10^{-2} mol). Whilst stirring, 3.3 M sodium hydroxide (15 mL) was added to the mixture at 0 °C. To the mixture, 2-Bromopropionic acid was added dropwise (7.6 g, 5.0×10^{-2} mol). The reaction was left to stir for 16 hours at room temperature, after which the pH of the solution was adjusted from pH 7 to pH 1 by using 2 M HCl. Extraction of the product, was achieved with diethyl ether (2 x 200 mL). Sodium hydroxide solution was used to extract product from diethyl ether (25 g in 25 mL H_2O, 2 x 50 mL). 1 M HCl was used to adjust the pH to 3. Diethyl ether was used to extract the product from the acidic solution (200 mL). The organic phase was dried over anhydrous magnesium sulphate and the solvent was removed under reduced pressure. The product was recrystallized from hexane. White crystals were obtained.[33,34] The purity of ***Compound A*** was > 98 % by ^{1}H NMR with a yield of 87 %.

NMR spectroscopy peak assignments for Compound A

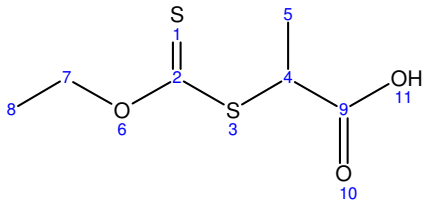

^{1}H NMR (300 MHz, $CDCl_3$) ppm
10.45, s, 1H (11)
4.71 – 4.56, q, 2H (7)
4.41, q, 1H (4)
1.60, d, 3H (5)
1.47 – 1.36, t, 3H (8)

^{13}C NMR (75 MHz, $CDCl_3$) ppm: 211.21 (2), 177.51 (9), 70.21 (7), 46.49 (4), 16.18 (5), 13.30 (8).

3.2.3.1.2) Synthesis of Succinimide CTA(Compound B)

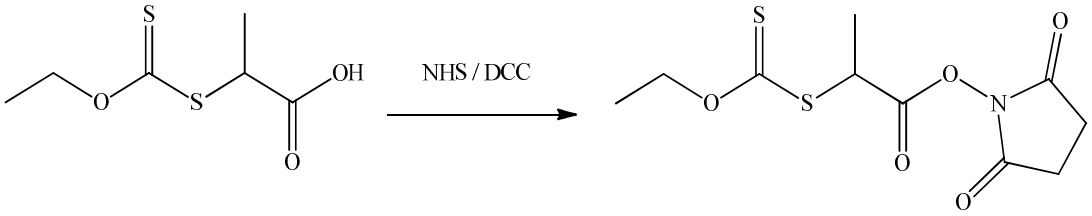

Scheme 3.2: Synthetic route for Compound B.

The xanthate chain transfer agent (***Compound A***) (2.09 g, 0.011 mol) was dissolved in 200 mL chloroform. The reaction mixture was cooled to 0 °C and flushed with argon for 30 minutes. DCC (2.27 g, 0.011 mol) and NHS (1.27 g, 0.011 mol) were added. The reaction was left to proceed at room temperature for 22 – 24 hours. The reaction mixture was filtered and the solvent removed under reduced pressure. A minimal amount of ethyl acetate was added to the reaction flask. The mixture was filtered and the solvent removed under reduced pressure.[35] The purity of ***Compound B*** was > 84 % by ^{1}H NMR and a yield of 40 % was obtained.

NMR spectroscopy peak assignments for Compound B

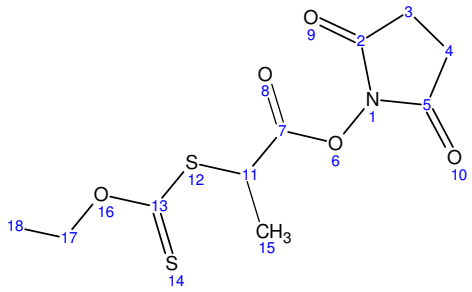

^{1}H NMR (400 MHz, $CDCl_3$)
4.75 – 4.55 ppm, m, 3H, (17,11)
2.88 – 2.69 ppm, m, 4H, (3,4)
1.70 ppm, d, 3H, (15)
1.49-1.48 ppm, t, 3H, (18)

^{13}C NMR (75 MHz, $CDCl_3$) ppm: 209.85 (13), 168.72 (7), 167.54 (5,2), 70.91 (17), 44.15 (11), 25.40 (3,4), 16.68 (15), 13.49(18)

3.2.3.2) Polymerization

The following equation was used to determine the theoretical molecular weight. AIBN: CTA ratio was kept at 1:5 (mol/mol). The assumption was made that the CTA is completely consumed during the polymerization and all polymer chains are initiated by the CTA.

$$M_{n(Theoretical)} = \frac{\alpha[M]o}{[CTA]} * M_{w(Monomer)} + M_{w(CTA)}$$

$M_{n(Theoretical)}$ – Molar mass targeted when performing the polymerization

[M]o – Initial monomer concentration

[CTA] – Initial concentration of the CTA (***Compound B***)

α – Monomer conversion

$M_{w(Monomer)}$ – Molar mass of monomer

$M_{w(CTA)}$ – Molar mass of CTA

3.2.3.2.1) Polymerization of NVP with Succinimide CTA

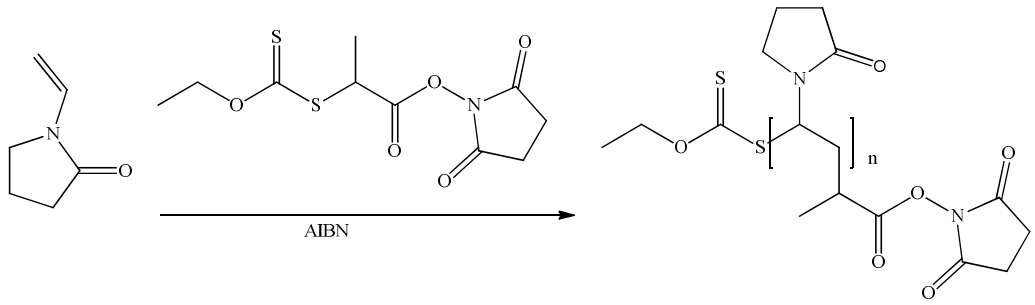

Scheme 3.3: Synthetic route for polymerization of NVP with Succinimide CTA.

Freshly distilled NVP (10 g, 0.09 mol), AIBN (0.033 g, 0.21 mmol) and ***Compound B*** (0.283 g, 1.03 mmol) were carefully weighed into a 100 mL pear-shaped Schlenk flask containing a magnetic stirrer. Freeze-pump-thaw cycle was repeated four times, after which the flask was filled with argon. The flask was placed in an oil bath and the polymerization was allowed to take place at 60 °C for 5 hours. PVP-succinimide (the product) was dissolved in DCM and precipitated from diethyl ether (2 x), filtered, dried under vacuum and kept under an argon atmosphere.

3.2.3.3) Post-polymerization reactions

3.2.3.3.1) Post-polymerization modification of PVP-Succinimide (Aminolysis)

The reaction between a thiocarbonyl-thio compound and an amine is a rapid reaction that yields thiols and disulfides.[36] In this study, advantage was taken of disulfide formation because it would

result in telechelic amino-functional PVP after deprotection of the succinimide functional group.[37] Furthermore the synthesis of polymer chains containing a reducible disulfide moiety provides exciting alternatives when it comes to biodegradable polymers.[3] A common aminolysis procedure was applied as shown in *Scheme 3.5*.[36,37]

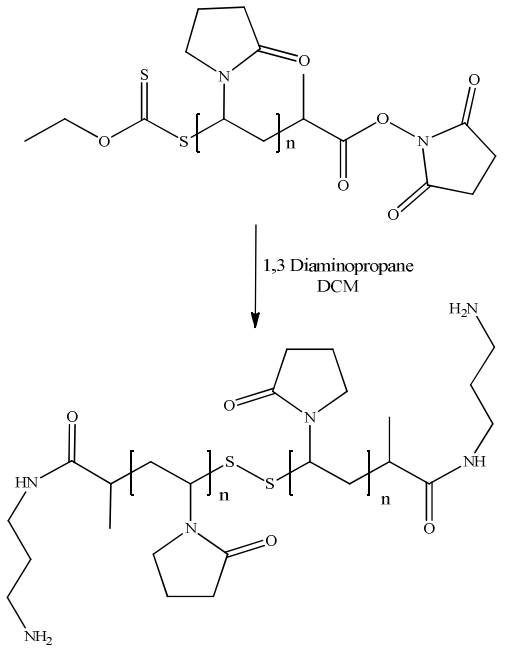

Scheme 3.4: Synthetic route for the aminolysis of PVP.

(2.6 g, 3.46x10^{-4} mol) PVP-Succinimide ($M_{n(NMR)}$ 15,000 g/mol, $M_{n(SEC)}$12,500 g/mol, Đ = 1.23) was dissolved in 50 mL dry DCM. Note that the mole calculations are based on the number of end groups (xanthate and succinimide). The solution was heated to 40 °C. 1,3-Diaminopropane (0.77 g, 0.0104 mol) was added dropwise. The reaction was left to proceed at 40 °C for 14 hours. The reaction was stopped and the precipitate filtered off and discarded. The product was dissolved in DCM and precipitated from diethyl ether (2 x). The product was dissolved in distilled water at 40 °C, placed into a slide-a-lyzer cassette (MWCO: 2000 g/mol) and dialyzed for 48 hours, with the water being changed every 8 – 12 hours. The polymer was obtained via freeze drying.

3.2.3.4) Modification of P(STY-*alt*-MAnh)

In an attempt to eliminate solvent from the gel synthesis, it was desirable to make use of water soluble P(STY-*alt*-Manh). Although P(STY-*alt*-Manh) is readily soluble in water when the MAnh units have been ring-opened, for the purpose of this study the majority of the MAnh units had to

remain intact (ring-closed) for reaction with the amine-functionalities of the modified PVP. In an alternative modification, advantage was taken of the solubility properties of PEG. Attachment of PEG onto STY would dramatically improve the water-solubility of P(STY-*alt*-MAnh) whilst keeping all MAnh units intact for reaction with $PVP(NH_2)_2$.

3.2.3.4.1) Synthesis of PEG-polystyrene maleic anhydride

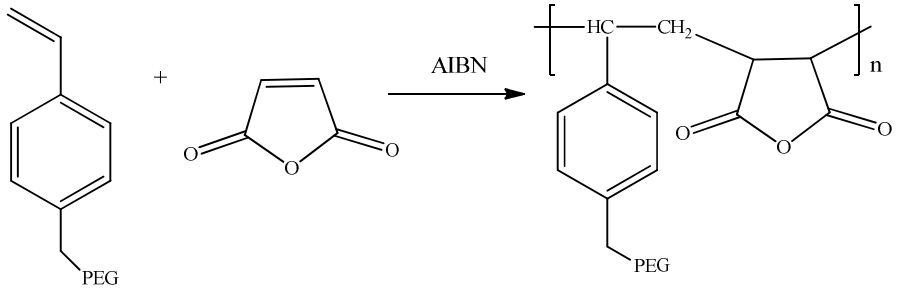

Scheme 3.5: Reaction scheme for the synthesis of P[(PEG-STY)-alt-MAnh].

p-Vinyl benzyl-poly(ethylene glycol) (1.5 g, 0.0023 mol) was weighed into a dry100 mL Schlenk flask. Freshly recrystallized maleic anhydride (0.22 g, 0.0023 mol) and AIBN (0.0037 g, $2.25x10^{-5}$ mol) were added to 10 mL 1,4 - dioxane. The mixture was degassed via four freeze-pump-thaw cycles, after which the flask was filled with argon. The reaction was left to proceed for 48 hours at 75 ºC. The product was precipitated in ice-cold diethyl ether. The solvent was removed and the P[(PEG-STY)-*alt*-MAnh] was kept under an argon atmosphere.

3.2.3.5) Gels

3.2.3.5.1) Gel formation of $PVP(NH_2)_2$and P(STY-alt-MAnh)

$PVP(NH_2)_2$ (0.060 g, $8.0x10^{-6}$ mol) was dissolved in 82 µL DMF and P(STY-*alt*-MAnh) (0.016 g, $8.0x10^{-5}$ mol (MAnh)) was dissolved in 242 µL DMF respectively. The $PVP(NH_2)_2$ solution was added to the P(STY-*alt*-MAnh) solution. Gel formation was instantaneous. Various molar ratios of the reactants and concentrations were investigated. Swelling studies were done on the gels obtained. See *Table 3.1* for reaction conditions. *Figure 3.1* shows an image of the gel.

Table 3.1: Summary of selected hydrogel reaction conditions

Gel	Mass PVP	[a)]Mol $PVP(NH_2)_2$	Mass PSTY-alt-Manh	Mol Manh	Solid wt% in solvent	[b)]Volume µL	Gel Y/N
1	0.060	8.000E-06	0.016	8.000E-05	20	323	N
2	0.060	8.000E-06	0.016	8.000E-05	25	242	Y
3	0.060	8.000E-06	0.016	8.000E-05	33	164	Y
4	0.050	6.667E-06	0.027	1.333E-04	20	326	N
5	0.050	6.667E-06	0.027	1.333E-04	25	244	Y
6	0.050	6.667E-06	0.027	1.333E-04	33	165	Y
7	0.090	6.000E-06	0.018	8.911E-05	20	458	[c)]Y
8	0.090	6.000E-06	0.018	8.911E-05	25	343	Y
9	0.090	6.000E-06	0.018	8.911E-05	33	232	Y
10	0.055	3.687E-06	0.011	5.530E-05	33	157	Y
11	0.200	1.333E-05	0.040	2.000E-04	33	488	Y
12	0.055	3.687E-06	0.011	5.530E-05	33	131	Y
13	0.055	3.687E-06	0.011	5.530E-05	33	123	Y
14	0.055	1.843E-05	0.037	1.843E-04	33	199	Y
15	0.055	1.843E-05	0.056	2.765E-04	33	239	Y
16	0.055	1.843E-05	0.074	3.687E-04	33	279	Y

*Note: a) M_n of $PVP(NH_2)_2$ Gels 1 - 14 was 15,000 g/mol, whereas M_n of $PVP(NH_2)_2$ Gels 15 - 16 was 3,000 g/mol. The molecular weight of one P(STY-*alt*-MAnh) unit was used for all calculations (202 g/mol). b) Gels 1 - 12 and 15 - 16was formed in DMF. Gel 13 was formed in 1,4 - dioxane and Gel 14 in DMSO. c) Gel 7 formed after 24 hours.*

Figure 3.1: Gel of $PVP(NH_2)_2$ and P(STY-alt-MAnh).

3.2.3.5.2) Gels of P[(PEG-STY)-alt-MAnh] and $PVP(NH_2)_2$

$PVP(NH_2)_2$ (0.010 g, $4x10^{-6}$ mol) was dissolved in 40 µL distilled water and 56 µL distilled water was used to dissolve P[(PEG-STY)-*alt*-MAnh] (0.040 g, $1.98x10^{-4}$ mol). The $PVP(NH_2)_2$ solution

was added to the P[(PEG-STY)-*alt*-MAnh] solution. No gel was obtained. When the same reaction was repeated in DMF, a gel was obtained.

3.2.3.6) Swelling studies procedure

Once the gels were formed, the gels were removed from the vials and dried in a dessicator overnight. The dry gel was weighed and placed in distilled water or PBS. The hydrogel was initially weighed every 5 minutes for the first hour and then at regular intervals until equilibrium was reached. Note that gels are only referred to as hydrogels once the gel has proven to absorb and retain fluid.

References

(1) Lima, V.; Jiang, X.; Brokken-Zijp, J.; Schoenmakers, P. J.; Klumperman, B.; Van Der Linde, R. *J. Polym. Sci., Part A: Polym. Chem.***2005**, *43*, 959.

(2) Tasdelen, M. A.; Kahveci, M. U.; Yagci, Y. *Prog. Polym. Sci.***2011**, *36*, 455.

(3) You, Y.-Z.; Manickam, D. S.; Zhou, Q.-H.; Oupick, D. *Biomacromolecules.***2007**, *8*, 2038.

(4) Boyer, C.; Granville, A.; Davis, T. P.; Bulmus, V. *J. Polym. Sci., Part A: Polym. Chem.***2009**, *47*, 3773.

(5) Boyer, C.; Liu, J.; Bulmus, V.; Davis, T. P.; Barner-Kowollik, C.; Stenzel, M. H. *Macromolecules.***2008**, *41*, 5641.

(6) Kopecek, J.; Yang, J. *Polym. Int.***2007**, *56*, 1078.

(7) Baier, R. E.; Zisman, W. A. *Macromolecules.***1970**, *3*, 70.

(8) Bosma, M.; Vorenkamp, E. J.; ten Brinke, G.; Challa, G. *Polymer.***1988**, *29*, 1694.

(9) Chaterji, S.; Kwon, I. K.; Park, K. *Prog. Polym. Sci.***2007**, *32*, 1083.

(10) Drotleff, S.; Lungwitz, U.; Breunig, M.; Dennis, A.; Blunk, T.; Tessmar, J.; Göpferich, A. *Eur. J. Pharm. Biopharm.***2004**, *58*, 385.

(11) Furth, M. E.; Atala, A.; Van Dyke, M. E. *Biomaterials.***2007**, *28*, 5068.

(12) Gupta, K. M.; Barnes, S. R.; Tangaro, R. A.; Roberts, M. C.; Owen, D. H.; Katz, D. F.; Kiser, P. F. *J. Pharm. Sci.***2007**, *96*, 670.

(13) Jeong, J.-H.; Byoun, Y.-S.; Lee, Y.-S. *React. Funct. Polym.***2002**, *50*, 257.

(14) Koul, V.; Srivastav, A.; Guha, S. K. *Contraception.***1998**, *58*, 227.

(15) Mishra, G.; McArthur, S. L. *Langmuir.***2010**, *26*, 9645.

(16) Pound, G.; McKenzie, J. M.; Lange, R. F. M.; Klumperman, B. *Chem. Commun.***2008**, 3193.

(17) Sasai, Y.; Kondo, S.; Yamauchi, Y.; Kuzuya, M. *J. Photopolym. Sci. Technol.***2010**, *23*, 595.

(18) Sasai, Y.; Kondo, S.; Yamauchi, Y.; Kuzuya, M. *J. Photopolym. Sci. Technol.***2009**, *22*, 503.

(19) Shulkin, A.; Stöver, H. D. H. *J. Membr. Sci.***2002**, *209*, 421.

(20) Tang, C.; Ye, S.; Liu, H. *Polymer.***2007**, *48*, 4482.

(21) van Hest, J. C. M.; Tirrell, D. A. *Chem. Commun.***2001**, 1897.

(22) Ladaviere, C.; Delair, T.; Domard, A.; Pichot, C.; Mandrand, B. *Polym. Degrad. Stab.***1999**, *65*, 231.

(23) Maeda, H. *Adv. Drug Delivery Rev.***2002**, *6*, 181.

(24) Maeda, H.; Takeshita, J.; Kanamaru, R. *Int. J. Pept. Protein Res.***1979**, *14*, 81.

(25) Maeda, H.; Ueda, M.; Morinaga, T.; Matsumoto, T. *J. Med. Chem.***1985**, *28*, 455.

(26) Mishchenko, V. F.; Zubov, V. A.; Yevdokimov, V. A. *Polymer Science.***1983**, *25*, 2254.

(27) Carstens, M. G.; van Nostrum, C. F.; Ramzi, A.; Meeldijk, J. D.; Verrijk, R.; de Leede, L. L.; Crommelin, D. J. A.; Hennink, W. E. *Langmuir.***2005**, *21*, 11446.

(28) Monfardini, C.; Veronese, F. M. *Bioconjugate Chem.***1998**, *9*, 418.

(29) Dinç, C. Ö.; Kibarer, G.; Güner, A. *J. Appl. Polym. Sci.***2009**, *117*, 1100.

(30) Gullapalli, R. P. *J. Pharm. Sci.***2010**, *99*, 4107.

(31) Karakoti, A. S.; Das, S.; Thevuthasan, S.; Seal, S. *Angew. Chem.***2011**, *50*, 1980.

(32) Yin, X.; Stover, H. D. H. *Macromolecules.***2002**, *35*, 10178.

(33) Pound, G. PhD, University of Stellenbosch, 2008.

(34) Meinjohanns, E.; Meldal, M.; Paulsen, H.; Bock, K. *J. Chem. Soc.***1995**, 405.

(35) Bathfield, M.; D'Agosto, F.; Spitz, R.; Charreyre, M.; Delair, T. *J. Am. Chem. Soc.***2006**, *128*, 2546.

(36) Castro, E. A. *Chem. Rev.***1999**, *99*, 3505.

(37) Cleland, W. W. *Biochemistry.***1964**, *3*, 480.

Chapter 4

4.1) Results and Discussion

In this chapter, PVP-succinimide and telechelic amino-functionalized PVP ($PVP(NH_2)_2$) synthesized as described in *Chapter 3* were characterized by means of ^1H NMR spectroscopy, UV-vis spectroscopy, ATR-FTIR spectroscopy, SEC and MALDI-TOF-MS. The CTAs synthesized and used for the synthesis of these polymers were characterized by means of ^1H and ^{13}C NMR spectroscopy. All the gels obtained were characterized by means of ATR-FTIR spectroscopy.

4.1.1) Chain transfer agents

The acid-functional xanthate CTA (***Compound A***) was successfully synthesized in high yield (87 %) with high purity as shown in *Chapter 3*. NaOH is used in the workup of the reaction in order to deprotonate 2-bromopropionic acid ensuring that the xanthate salt does not get protonated. Protonation of the xanthate salt results in decomposition of the xanthate, which results in lower yields of the product. Unreacted xanthate salt is removed from the reaction mixture by a dilute solution of hydrochloric acid. The structure of the xanthate CTA was confirmed via ^1H and ^{13}CNMR spectroscopy.

Polymerization of NVP with this CTA resulted in very low monomer conversions as a result of NVP dimer formation together with various other side reactions.[1] For this reason, the polymerization could not be carried out with unprotected carboxylic acid functionality as this group was suspected to be the reason for the side reactions and dimer formation.[2] Furthermore, a CTA with an acid end-group rapidly undergoes esterification with NVP, and therefore polymerization was performed with the CTA's corresponding ester (***Compound B***).[2]

Synthesis of the succinimide CTA (***Compound B***) proved to be poorly reproducible. Dicyclohexyl-urea (DCU) formed as a result of the DCC coupling reaction. DCU is insoluble in most organic solvents, but could not be completely removed after filtration. *Compound B* degraded in a silica column. The structure of the succinimide CTA was confirmed by means of ^1H and ^{13}CNMR spectroscopy.[3,4] The purity was > 84 % as determined by ^1H NMR and the yield obtained was 40 %.

4.1.2) General procedure for polymerization

Polymerization temperature and reaction time were carefully chosen. The optimal temperature was found to be 60 ºC. Polymerizations were never left for longer than 6 hours in order to avoid any possible side reactions such as dimer formation.[2] During some of the reactions it was necessary to stop the reaction earlier due to a rapid increase in viscosity, which stalled mechanical stirring.

Polymer was precipitated from diethyl ether. In cases where the medium was too viscous, the polymer was diluted with DCM before precipitation. In general, most of the monomer was removed after two precipitations from diethyl ether.

It is important to point out that the reproducibility of NVP polymerizations is poor. Although reactions were run in the same manner, different results were obtained. Many reasons are suggested for this, one of which is the presence of oxygen. However, much care was taken to perform these reactions under inert conditions.[2]

4.1.3) Characterization of synthesized polymers

^{1}H NMR spectroscopy is particularly useful for the identification of the CTA present at the polymer chains-ends, especially for polymers with M_n< 10 000 g/mol. This was consequently used for the quantitative determination of the average molar mass of the polymer.

In the ^{1}H NMR of PVP-succinimide (*Figure 4.1),* the peak at 4.6 ppm was identified as the -OC**H$_2$**CH$_3$ on the Z-group of the CTA at 4.6 ppm (*Peak a*). This was used as a reference peak, and integrated to the number of protons of the -OC**H$_2$**CH$_3$ on the Z-group of the CTA. (In this case the peak area was normalized to a value of 2, to signify that it represents two protons.) The peak at 3.0 – 4.1 ppm (*Peak b*) represents the polymer backbone protons, *i.e.* three protons per monomer repeat unit. The ratio between the peaks was used as an indication of the average degree of polymerization. The peak at 4.3 – 4.4 ppm (*Peak c*) is also integrated with reference to the peak at 4.6 ppm in order to subtract any residual monomer. The latter is characteristic of -C**H$_2$**CHN on the lactam ring of PVP. The value obtained is then multiplied by the molar mass of one NVP unit (111 g/mol).

$$M_{n_{(Experimental)}} = \left\{\left[\frac{A_{3.0-4.1ppm}}{3}\right] - \frac{A_{4.3-4.4ppm}}{2}\right\} * 111 g/mol$$

Although NMR spectroscopy could not be used for the determination of the average molar mass of the PVP$(NH_2)_2$, it was a useful tool to confirm the removal of the xanthate peak after aminolysis. In *Figure 4.1*, the absence of the xanthate peak at 4.6 ppm in the bottom spectrum serves as proof that the xanthate moiety has been successfully removed by means of aminolysis.

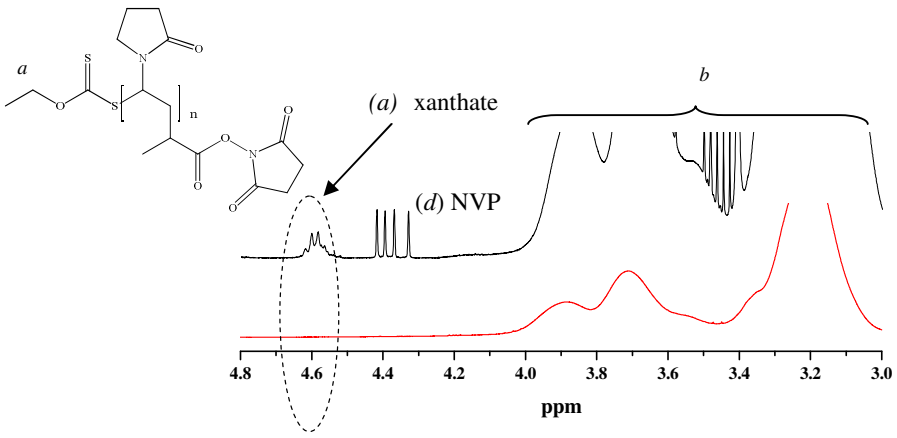

Figure 4.1: ^{1}H NMR comparison of the polymer before and after aminolysis.
Top spectrum: PVP with the xanthate end-group, before aminolysis. Bottom spectrum: PVP after aminolysis.

SEC was used to obtain additional information regarding the molar mass and molar mass distribution of the polymers that were synthesized. In SEC, the polymer is passed through a column and separated on the basis of hydrodynamic volume.[5]

Once the polymer has passed through the column, it is detected by a refractive index detector. The signal produced is proportional to the concentration of the eluting polymer. Due to the lack of suitable PVP standards to use for calibration, the values of average molar mass obtained from SEC are based on PMMA standards. The values obtained from SEC are therefore not true values, but rather relative to the standards used. As a result one cannot rely exclusively on SEC values in determining the molar mass of the polymers.

Although there was generally a good correlation between the SEC values and the M_n obtained from ^{1}H NMR, discrepancies in these values are not uncommon. One of the reasons is that often there is overlap of the polymer peak, with solvent and monomer residue in the ^{1}H NMR spectrum. As a result ^{1}H NMR integration values could easily be overestimated. Despite possible discrepancies, it is believed that the values are appropriate for evaluation purposes. Major discrepancies were only encounter with higher M_n polymers (> 10 000 g/mol). SEC results obtained

for polymers lower than 3,000 g/mol were in good agreement with those calculated from ^{1}H NMR spectra.

The SEC chromatograms obtained for PVP before and after aminolysis are shown in *Figure 4.2.* The overlap of the two distribution curves was expected, as the one corresponds to the polymer before modification and the other to the polymer after modification. Tailing toward the lower molar mass regions was attributed to chain breaking reactions.

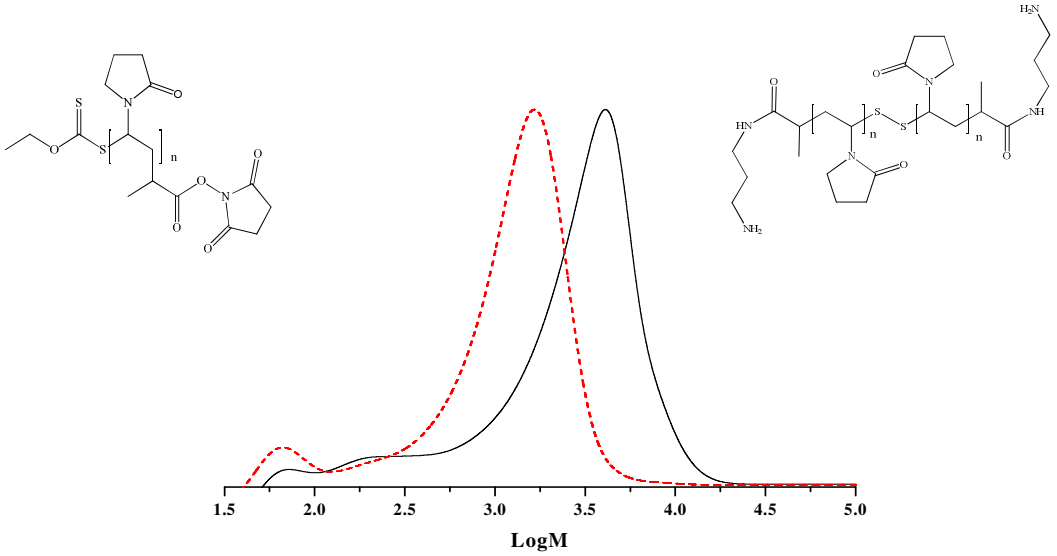

Figure 4.2: Molar Mass distribution of PVP and PVP(NH$_2$)$_2$.
Dotted line: Polymer before aminolysis. $M_{n(NMR)}$: 1500g/mol , $M_{n(SEC)}$: 1500g/mol, Đ = 1.18. Solid line: Polymer after aminolysis. $M_{n(SEC)}$: 3000g/mol, Đ = 1.32.

Broadening of the PVP(NH$_2$)$_2$ distribution was observed which was also reflected in an increase in dispersity. This was attributed to interaction of the amine functionalities with the column. Furthermore, it is possible that not all the polymer chains formed disulfide bridges, and as a result, there are some thiol functionalities present in the sample. The calculated molar mass was in good agreement with that of two chains linked via a disulfide bridge as there was a doubling of the molar mass of the PVP(NH$_2$)$_2$ compared to the succinimide-PVP. SEC also gave an indication of the control of the polymerization. All dispersities were < 1.4 indicating adequate control during polymerization.

Qualitatively, UV-Vis and ATR-FTIR spectroscopy were useful in comparing PVP-succinimide to the PVP(NH$_2$)$_2$. The xanthate functionality has a strong UV absorbance at 280 nm.[6] A significant decrease of absorbance in this region would indicate the removal of the xanthate. In *Figure 4.3* the UV-vis spectra of PVP-succinimide and PVP(NH$_2$)$_2$ are shown. The bottom spectrum of the

$PVP(NH_2)_2$ shows a drastic decrease in absorption at 280 nm. This serves as further proof that the xanthate end-group has indeed successfully been removed from the succinimide-PVP by means of aminolysis to render $PVP(NH_2)_2$.

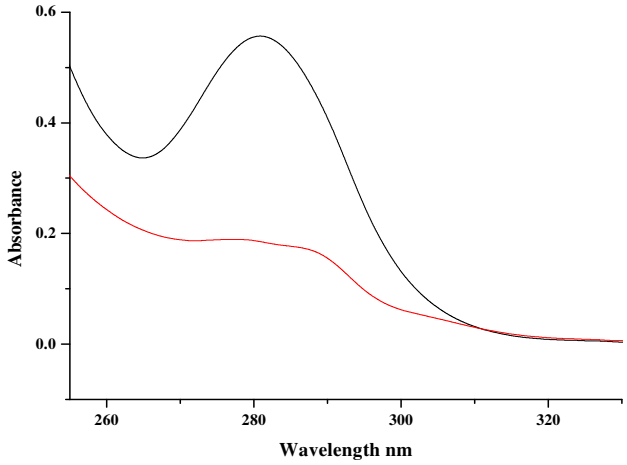

Figure 4.3: UV-vis spectra of PVP-succinimide vs $PVP(NH_2)_2$ in chloroform.
Top spectrum: PVP-succinimide still containing the xanthate functionality. Bottom spectrum: $PVP(NH_2)_2$.

In *Figure 4.4,* the ATR-FTIR spectra of PVP-succinimide and $PVP(NH_2)_2$ are shown. Peaks of particular interest were those of the activated ester as well as the xanthate functionality. υ(C=O) vibrations present due to the lactam-rings of PVP exhibit a strong absorbance between 1550 – 1750 cm^{-1}. This makes differentiation between the starting compound and product difficult.

Aminolysis of the PVP-succinimide results in the removal of the activated ester group present at 1748 cm^{-1}. This is clearly visible in the bottom spectrum. The xanthate end-group present on the PVP-succinimide has a strong absorbance at 1046 cm^{-1}. The absence of these two absorbencies in the spectra of $PVP(NH_2)_2$ further serves as proof that the end-functionalization was successful. It is important to note that this is not a quantitative measurement and can only be used in conjunction with other characterization techniques.[7,8]

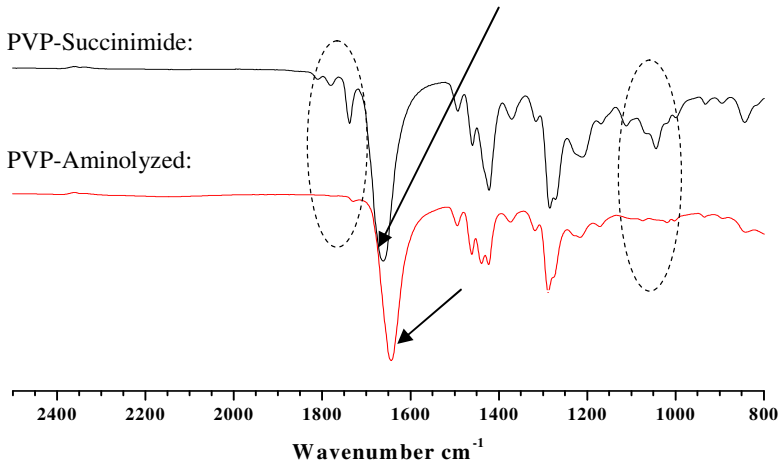

Figure 4.4: ATR-FTIR spectrum of PVP vs PVP(NH$_2$)$_2$.
Top spectrum: PVP-succinimide. Bottom spectrum: PVP(NH$_2$)$_2$.

As further proof of successful modification, MALDI-ToF-MS was recorded for both PVP-succinimide and PVP(NH$_2$)$_2$ *(Figures 4.5 and 4.6).* Ionization results in the polymer chains being separated by absolute mass over charge (m/z). In literature there are various cases where MALDI-ToF-MS was used to identify various end groups on PVP with $M_n < 10\,000$ g/mol.[9-13]

The mass spectra of PVP-succinimide displayed numerous fragmentation patterns. This was expected for PVP that contained the xanthate functionality as these chain ends easily cleave upon UV irradiation and ionization. The reason for this is that ionization takes place close to the absorption wavelength of the C=S bond. In *Figure 4.5 (c) and 4.6 (c)*, there is a comparison between the isotopic patterns obtained experimentally and those obtained theoretically. As shown there is a very good correlation between the theoretical isotopic patterns and those obtained experimentally for both PVP-succinimide and PVP(NH$_2$)$_2$.

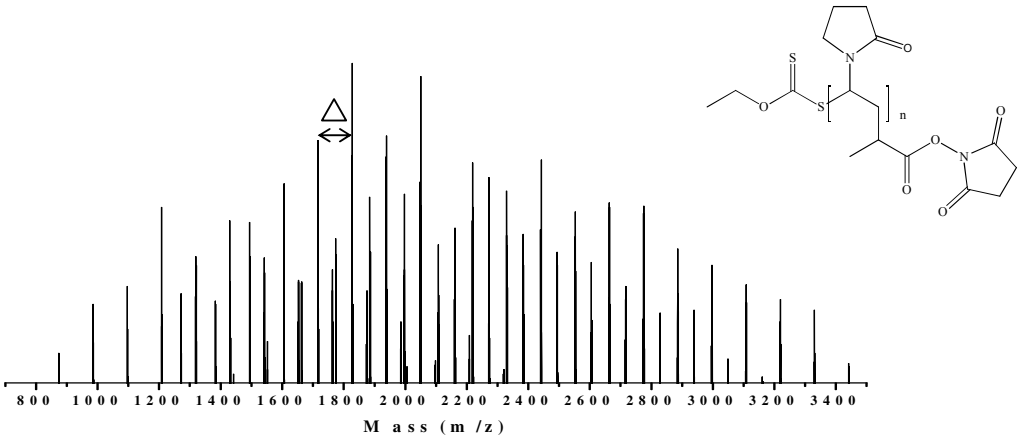

Figure 4.5 (a): Experimental MALDI-ToF-MS spectrum for PVP-succinimide.

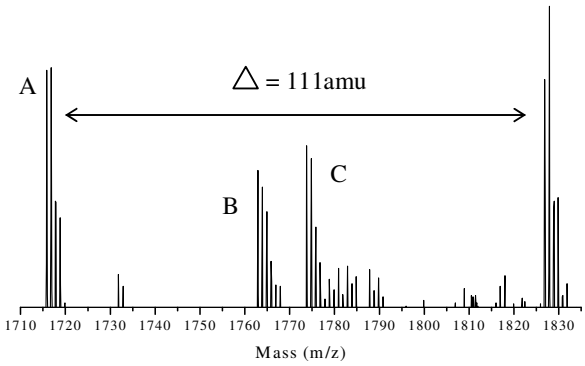

Figure 4.5 (b): MALDI-ToF-MS spectrum for PVP-succinimide, enlargement of region 1710-1830 amu.

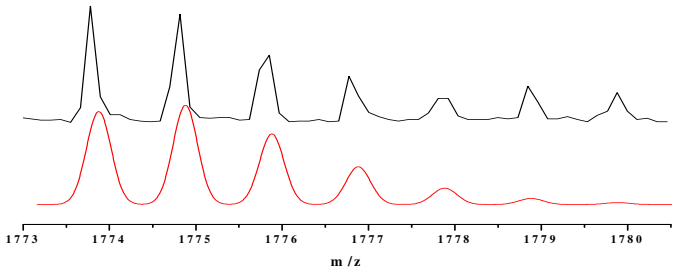

Figure 4.5(c): MALDI-ToF-MS spectrum for PVP-succinimide, experimental vs. theoretical spectrum obtained.

Top spectrum - Experimental spectrum obtained between 1773-1781amu.
Bottom spectrum - Theoretical spectrum obtained between 1773-1781amu.

The mass spectra obtained for $PVP(NH_2)_2$ matched calculations for two PVP chains with a disulfide bridge linker. *Table 4.1* contains all structures of the isotopic fragmentations identified.

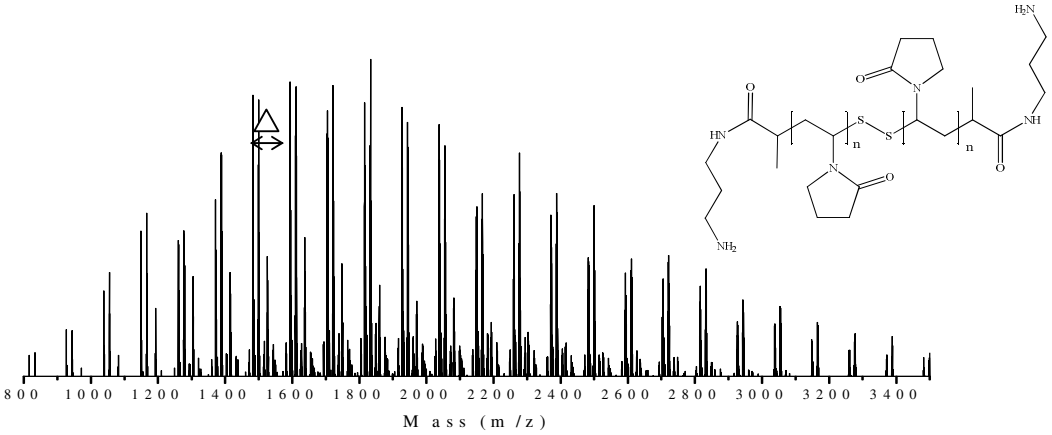

Figure 4.6 (a): MALDI-ToF-MS spectrum for $PVP(NH_2)_2$.

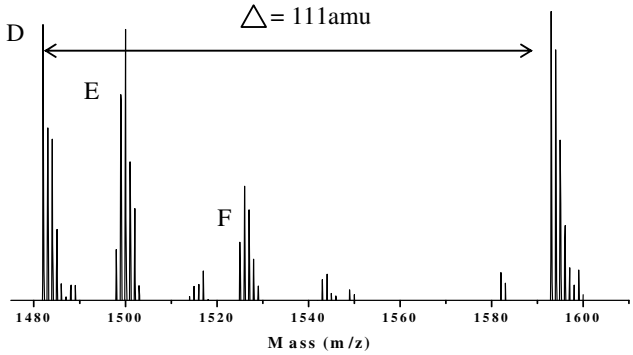

Figure 4.6(b): MALDI-ToF-MS spectrum for $PVP(NH_2)_2$, enlargement of region 1482 – 1593 amu.

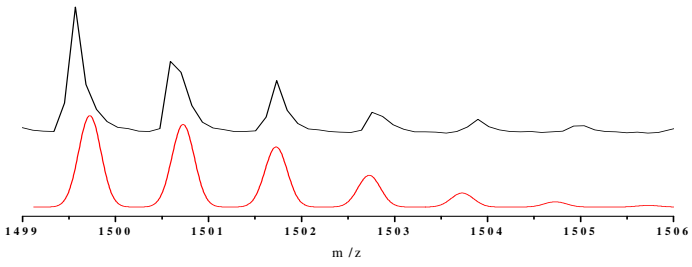

Figure 4.6(c): MALDI-ToF-MS spectrum for $PVP(NH_2)_2$, experimental vs theoretical spectrum
Top spectrum - Experimental spectrum obtained between 1499-1506amu.
Bottom spectrum - Theoretical spectrum obtained between 1499-1506amu.

Table 4.1: Fragmentation patterns for MALDI-ToF-MS in Figure 4.5 (b) and 4.6 (b)

Peak	Structure	Theoretical Mn	Experimental Mn
A	$C_3H_5OS_2(C_6H_9NO)_{14}H$ Or $C_3H_5OS_2(C_6H_9NO)_{13}C_3H_5O_2K^+$	1716.91 g/mol OR 1716.89 g/mol	1716.84 g/mol OR 1716.82 g/mol
B	$CHOS_2(C_6H_9NO)_{14}C_3H_4O_2H$	1761.90 g/mol	1762.87 g/mol
C	$C_3H_5OS_2(C_6H_9NO)_{13}C_7H_8O_4NK^+$	1774.88 g/mol	1774.81 g/mol
D	$(NHOC_2H_4)_2(C_6H_9NO)_{11}S_2K^+$	1481.89 g/mol	1482.00 g/mol
E	$(C_3H_9N_2)_{20}$	1500.49 g/mol	1500.03 g/mol
F	$(HOC_2H_4)_2(C_6H_9NO)_{12}S_2$	1525.79 g/mol	1526.04 g/mol

From this it was concluded that the conversion of PVP-succinimide to aminolyzed PVP was successful as all characterization techniques were in good agreement. M_n values of the aminolyzed PVP were double the M_n values of those calculated for the PVP-succinimide. This is shown in *Table 4.2* for selected polymerization reactions. As PVP with a molar mass above 5000 g/mol cannot be properly ionized, MALDI-ToF-MS was only used for the lower M_n polymers.

Table 4.2: Summary of selected polymers used for modification

	PVP-Succinimide				*PVP-aminolyzed*		
	$M_{n(NMR)}$ g/mol	$M_{n(SEC)}$ g/mol	Đ	$M_{p(MALDI-ToF-MS)}$ g/mol	$M_{n(SEC)}$ g/mol	Đ	$M_{n(MALDI-ToF-MS)}$ g/mol
1	7,500	12,071	1.18	NA	17,362	1.32	NA
2	7,500	12,071	1.18	NA	15,657	1.50	NA
3	1,500	1,555	1.18	1,690	3,144	1.38	3,280
4	2,240	2,533	1.37	2,380	3,803	1.74	3,940
5	1,720	1,779	1.23	1,860	3,400	1.60	3,540

4.1.4) Modification of P(STY-*alt*-MAnh)

4.1.4.1) Synthesis of [P(PEG-STY)-alt-MAnh]

P[(PEG-STY)-*alt*-MAnh] *(see Figure 4.7)* was soluble in distilled water after synthesis. Solubility lasted for about a week, after which the P[(PEG-STY)-*alt*-MAnh] was no longer soluble in water. However it was still soluble in 5 % ammonia solution. It is possible that there is hydrogen bonding taking place between the acid groups of the MAnh units and the PEG on the STY units. This

interaction would decrease water-polymer interaction significantly preventing the P[(PEG-STY)-*alt*-MAnh] to dissolve at lower pH values.[5] ATR-FTIR spectroscopy was used to characterize the insoluble P[(PEG-STY)-*alt*-MAnh].

In *Figure 4.8* the carbonyl peak of P[(PEG-STY)-*alt*-MAnh] at 1838 cm^{-1} (*I*) and 1774 cm^{-1} (*H*) in the bottom spectrum have shifted to a lower wavenumber at 1735 cm^{-1} (*C*) in the top spectrum. This suggests ring opening of MAnh units.[5,14] The absorbancies in both spectra at 2885 cm^{-1} (*B*) and 1452 cm^{-1} (*G*) are assigned to -OCH_3 on the PEG moiety, whereas the absorbance at 1089 cm^{-1} (*F*) is attributed to *para*-substituted aromatic group. The broad peak formation at 3200 – 3500 cm^{-1} (*A*) is recognized as –COOH formation due to ring opening of the MAnh units.

Table 4.3:ATR-FTIR spectroscopy assignments for P[(PEG-STY)-alt-MAnh][8]:

Peak	*Wavenumber (cm^{-1})*	*Peak*	*Wavenumber (cm^{-1})*
A	3200-3500 cm^{-1}	***F***	1089 cm^{-1}
B	2885 cm^{-1}	***G***	1452 cm^{-1}
C	1735 cm^{-1}	***H***	1774 cm^{-1}
D	1651 cm^{-1}	***I***	1838 cm^{-1}
E	1605 cm^{-1}	***J***	2885 cm^{-1}

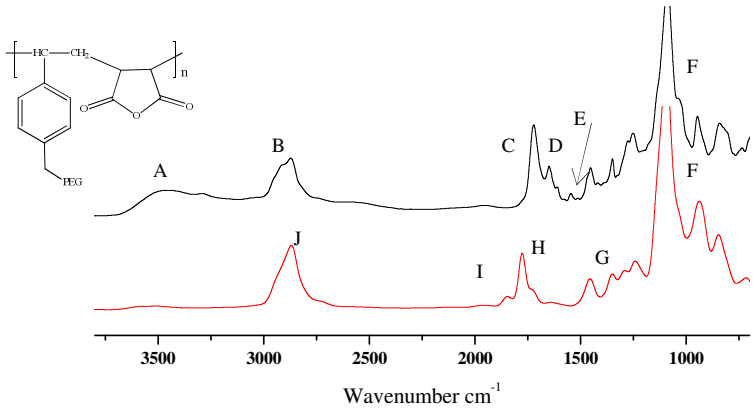

Figure 4.7: ATR-FTIR spectra of P[(PEG-STY)-alt-MAnh].
*Top spectrum: Insoluble*P[(PEG-STY)-*alt*-MAnh] *7days old.*
Bottom spectrum: Soluble P[(PEG-STY)-*alt*-MAnh] *straight after synthesis.*

The latter further supports the possibility of hydrogen bonding between the acid groups and PEG. If this is indeed the situation in the system, it further explains why the water insoluble P[(PEG-STY)-*alt*-MAnh] dissolved in ammonia solution, seen that the maleic acid was deprotonated reducing the H-bonding ability with PEG. Further studies will have to be done in order to confirm this possibility. However, the soluble P[(PEG-STY)-*alt*-MAnh] was used for gel synthesis.

4.1.5) Gels

4.1.5.1) PVP(NH$_2$)$_2$ and P[(PEG-STY)-alt-MAnh] gels

The gel formed from PVP(NH$_2$)$_2$ and P[(PEG-STY)-*alt*-MAnh] in DMF was characterized by means of ATR-FTIR spectroscopy. In *Figure 4.8*, there is clear evidence that both PVP(NH$_2$)$_2$ at 1640 cm^{-1} (*E*) and the PEG functionalities of the P[(PEG-STY)-*alt*-MAnh] at 2885 cm^{-1} (*B*) and 1089 cm^{-1} (*F*) are present in the gel. Furthermore -C=O of the MAnh is also evident in the gel sample at 1774 cm^{-1} (*C*) and 1838 cm^{-1} (*D*). As in the case with the previous gel there is a peak present at 1723 cm^{-1} suggesting symmetrical stretch of -C=O as a result of ring-opening due to reaction with an amine.[15] The assumption is made that the amide peak that is formed is masked by the absorption of the –C=O on the lactam ring of PVP.[5,16] Another possibility is that the cross-links that formed were physical and not chemical, and as a result one would not see the amide peak. However, the gel that formed was not soluble in DMF or water, so dissolution of the polymer chains did not take place.

Table 4.4: ATR-FTIR spectroscopy assignments for P[(PEG-STY)-alt-MAnh] hydrogels[8]:

Peak	*Wavenumber (cm^{-1})*	*Peak*	*Wavenumber (cm^{-1})*
A	3200-3500 cm^{-1}	***D***	1774 cm^{-1}
B	2885 cm^{-1}	***E***	1640 cm^{-1}
C	1838cm^{-1}	***F***	1089 cm^{-1}

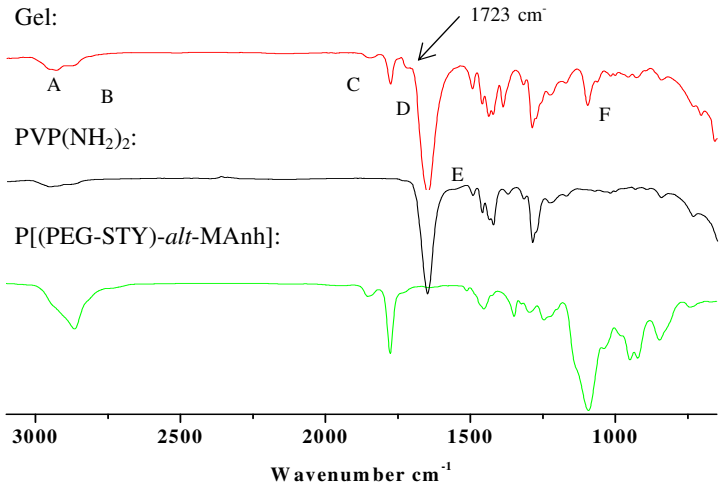

Figure 4.8: ATR-FTIR spectroscopy of P[(PEG-STY)-alt-MAnh] and PVP(NH$_2$)$_2$ gel.
Top spectra: Gel, Middle: PVP(NH$_2$)$_2$, Bottom: P[(PEG-STY)-alt-MAnh].

4.1.5.2) PVP(NH$_2$)$_2$ and unmodified P(STY-alt-MAnh) gels

ATR-FTIR spectroscopy was used to characterize these gels. Spectra obtained are shown in *Figure 4.9.* The spectrum recorded of the gel shows the characteristic peaks of both P(STY-*alt*-MAnh) at 1774, 1838 cm^{-1} (*D, C*) and PVP(NH$_2$)$_2$ at 1640 cm^{-1} (*E*).[7] In the spectrum of the gel, there is an absorbance at 1723 cm^{-1}, which suggests a -C=O symmetrical stretch as a result of ring-opening due to reaction with an amine.[15] The amide that forms should have an absorbance at 1680 cm^{-1}, however the –C=O on the lactam ring of PVP in the sample has strong absorbance between 1556 – 1700 cm^{-1}. It is possible that the PVP absorbance masks the absorbance of the amide that was expected and is therefore not visible in the spectra. However, the absence of the cyclic anhydride peaks at 1216 cm^{-1} and 918 cm^{-1} (*F*) indicates that ring-opening did indeed take place.

Table 4.5: ATR-FTIR spectroscopy assignments for P(STY-alt-MAnh)-PVP(NH$_2$)$_2$ gel.[8]

Peak	*Wavenumber (cm^{-1})*	*Peak*	*Wavenumber(cm^{-1})*
A	3200-3500 cm^{-1}	***D***	1774 cm^{-1}
B	2885 cm^{-1}	***E***	1640 cm^{-1}
C	1838cm^{-1}	***F***	1216,918 cm^{-1}

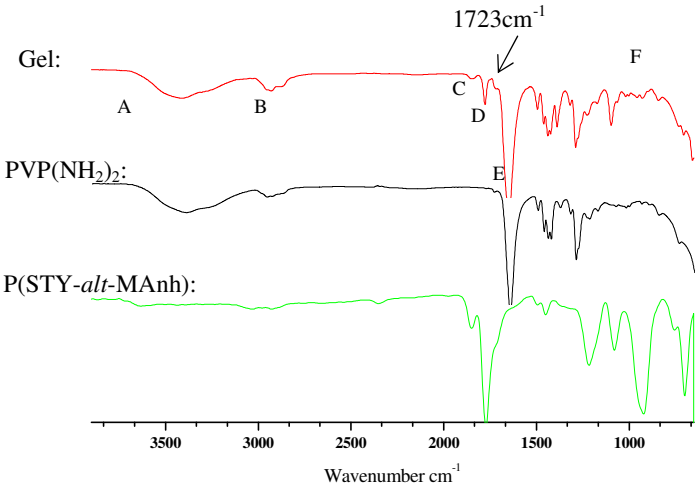

Figure 4.9: ATR-FTIR spectra of P(STY-alt-MAnh)-PVP(NH$_2$)$_2$ gel 5 *(see table 3.1).*

Various factors were investigated for their role in the synthesis of the gels. Firstly the role of molar ratios of the functional groups was investigated. If it is assumed that all the polymer chains are telechelic amino-functionalized, then every PVP chain will contain two amino functionalities, one at each chain-end. Per repeat unit of P(STY-*alt*-MAnh), there is one MAnh functionality for the

$PVP(NH_2)_2$ to react with, and as a result, per chain of PVP there need to be at least two MAnh units in order for a network to form successfully. MAnh was used in excess to ensure the all the amine functionalities could react and to promote intermolecular reaction over intra-molecular reaction.

The solid weight percentage (swt %) of the polymers in solution seemed to play the greatest role, especially with regard to the swelling ratio (see next section). Swt % indicates the mass of solids in the sample. Initially these values were varied in order to find the optimum value at which there would be enough solvent in order to dissolve the polymers, but also high enough polymer concentration to form a gel instantly. The swt % was varied from 20 %, and 25 % to 33 %. At swt % lower than these values the swelling ratio was not sufficient and the gelation took too long, up to a few weeks in the case of swt % of 5 %. At swt % higher than 33 %, there was not enough solvent to dissolve the polymers.

It was found that the higher the swt %, the shorter the gelation time. At 20 swt % it took up to 24 hours to obtain a gel. At swt % of 33 %, gelation was instantaneous. It was found that temperature did not significantly influence the gelation time of the gels. The solution was regarded as a gel once it did not flow down the side of the vial and remained stationary at the top when the vial was tilted. The gel swelled in water and/or PBS. The reaction was further performed in various organic solvents (DMSO and 1, 4-dioxane) which rapidly dissolve P(STY-*alt*-MAnh) and $PVP(NH_2)_2$. The use of these solvents was also successful in forming gels. The gels formed were placed in solvents (DMF, DMSO, 1,4-dioxane) which would rapidly dissolve $PVP(NH_2)_2$ and P(STY-*alt*-MAnh). None of the gels dissolved and merely swelled. This served as further proof that once the gels were formed, solvents which previously dissolved the polymers could not dissolve the gels. It was concluded that gel formation was successful.

4.1.6) Swelling studies performed on P(STY-*alt*-MAnh)-$PVP(NH_2)_2$ gels

Swelling studies involve the study of the increase in mass of a gel as a function of time due to liquid retention/absorption. This is an important characteristic due to the relationship that exists between the swelling of a gel in a given solvent and the nature of the solvent as well as the nature of the gel. The properties of gels are also dependant on the % water or biological fluid that can be absorbed by the gel. This in turn will determine the potential applications of the gel. In general, the

ionic structure of the gel plays a major role in these studies. The swelling of a gel is caused by the electrostatic repulsion of the ionic charges of the network. The more hydrophilic units available in the gel network, the greater the degree of swelling. Theoretically, the gel will absorb the fluid until equilibrium has been reached, after which the gel will no longer be able to absorb any fluid.[17-20] When the swelling studies are recorded, an exponential trend is expected, which will level off once equilibrium has been achieved. This constant swelling % at equilibrium is called the equilibrium water content (EWC %) (*Table 4.6)*. For a gel to have a similar fluid content to that of a living tissue, the EWC % has to be greater than the percentage water content of the body (ca.60 %).[21,22]

The percentage swelling was calculated as follow:

$$\%S = \frac{M_t - M_o}{M_o}\ x\ 100$$

M_t – Mass of the swollen gel at time t

M_o – Mass of the gel at time 0

The procedure used for the swelling studies introduced significant error. Before the gel was weighed it was blotted with filter paper. A graph was constructed to represent % swelling vs. time. From the graph in *Figure 4.10* it was evident that during the first 60 minutes the majority of fluid was absorbed. After that the absorption levelled off, the gels maintained this % swelling over a time period of up to 2 days.

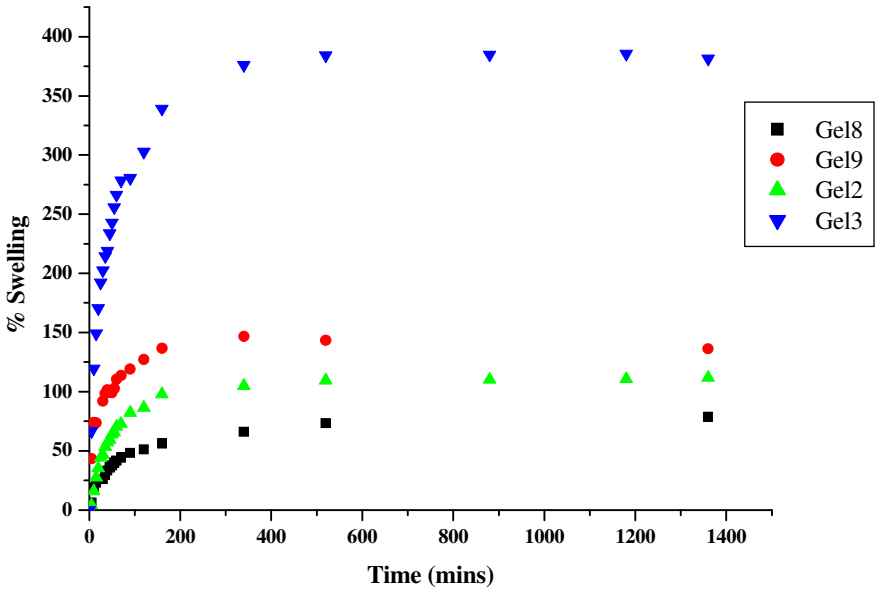

Figure4.10: Gel swelling studies done in distilled water at room temperature.
Gel 2,3,8 and 9 form Table 3.1.

The EWC % was calculated as follows:

$$\%EWC = \left(\frac{M_s - M_o}{M_o}\right) x\ 100$$

M_s *– Mass of swollen gel at equilibrium*

M_o *– Mass of the gel at time 0*

It is apparent from these studies that the % EWC obtained for the gels are sufficient for biological use, as all the gels described in this chapter have a % EWC of higher than 60 %.

Table 4.6: Summary of swelling studies for selected gels

Gel	Mol $(NH_2)_2$ x 10^6	Mol MAnh	Solid wt% in solvent	Volume (µL)	Dry weight (g)	Weight at equilibrium (g)	%EWC
2	8	$8.0x10^{-5}$	25 %	242	0.158	0.334	112 %
3	8	$8.0x10^{-5}$	33 %	163	0.099	0.334	381 %
8	6	$8.0x10^{-5}$	25 %	343	0.264	0.471	79 %
9	6	$8.0x10^{-5}$	33 %	232	0.206	0.486	136 %

When low molar mass $PVP(NH_2)_2$ (1500 g/mol) was used in the formation of the gels, the degree of swelling was 0 %. However, when these were placed in 5 % ammonia solution, the gels swelled

significantly. A possible explanation for this is, when the $PVP(NH_2)_2$ chains are shorter, the network is more densely cross-linked, rendering a mechanically more stable network, which is less prone to swelling. Furthermore, when lower molar mass $PVP(NH_2)_2$ is used, the weight fraction of PVP in the gel is smaller and as a result the hydrophilicity of the material is less. When the gels are placed in ammonia solution, all the unreacted MAnh units are opened, increasing the hydrophilicity. This allows low molar mass $PVP(NH_2)_2$ gels to swell.

The degree of swelling in distilled water was compared to the degree of swelling in 5 % ammonia solution. There was a remarkable difference as seen in *Figure 4.11*. The same gel had a swelling ratio of up to 750 % in 5 % ammonia compared to 365 % in distilled water. The reason for this was attributed to the fact that the ammonia solution further opens any unreacted maleic anhydride rings on the P(STY-*alt*-MAnh), increasing the hydrophilic nature of the gel, thereby increasing the amount of water that can be taken up and retained by the gel. Another reason presented for this was that MAnh units are hydrolyzing regardless of the presence of ammonia. The ammonia could form a salt (i.e. deprotonate the acids) and thereby increase the swelling as a result of charge repulsion.

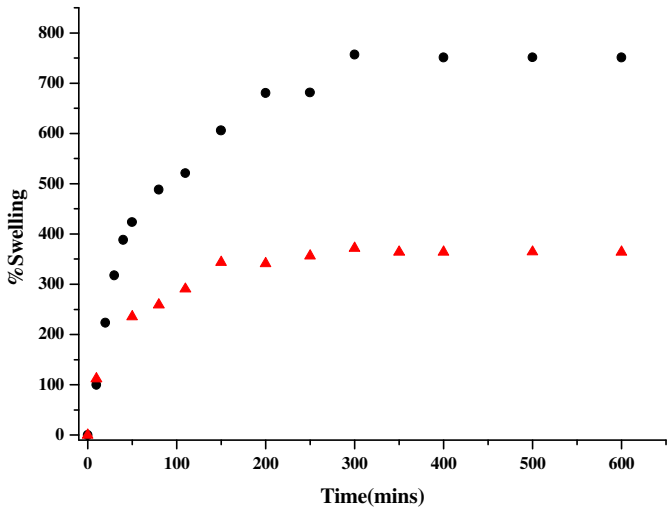

Figure 4.11: Gel swelling studies done in distilled water vs 5 %ammonia solution at room temperature for gel3.
Top line: Swelling profile of gel in 5 % ammonia solution. Bottom line: Swelling profile of the same gel in distilled water.

4.2) Conclusions

A method for preparing telechelic amino-functionalized PVP with good control over molecular weight and dispersity was successfully developed. All polymers synthesized in this study were meticulously characterized by ^{1}H NMR spectroscopy in conjunction with MALDI-ToF-MS, SEC, UV-vis and ATR-FTIR spectroscopy.

PVP$(NH_2)_2$ was effectively cross-linked with P(STY-*alt*-MAnh) resulting in a gel that was characterized by means of ATR-FTIR spectroscopy. The gels were placed in water, DMF, DMSO and 1, 4 - dioxane. None of these solvents dissolved the polymeric network, serving as proof that a gel was obtained. The ability of the gels to absorb and retain water was investigated by means of swelling studies with promising results for biological applications. When the gels were left in water for longer periods of up to 6 – 12 months, very little to no degradation was observed. However, it was observed that the gels still absorbed fluid over these prolonged periods. Consequently the gel network became weaker and as a result started breaking apart. There were however still no signs that the gel was dissolving. In further studies it would be valuable to establish the point where the hydrogel becomes mechanically weak during fluid uptake.

Although PVP$(NH_2)_2$ dissolves in less harmful solvents like water, P(STY-*alt*-MAnh) is not water soluble in its ring-closed state. The solvent of choice was therefore DMF for most of the gels. This dissolved both compounds rapidly. However, this is not ideal for the purpose of this project. DMF, as with many organic solvents, is toxic and carcinogenic. The ideal case would be to develop a gel that could form and swell in water in order to eliminate the use of toxic solvents, thereby automatically enhancing the biocompatibility of the gels.

P[(PEG-STY)-*alt*-MAnh] was readily soluble in water soon after synthesis, however when reacted with PVP$(NH_2)_2$ no gel was obtained in water, although a gel was obtained in DMF. The reason presented for this is that the MAnh moieties had been hydrolyzed in the aqueous solution before the PVP$(NH_2)_2$ solution was added. Future work would include the use of Raman spectroscopy in order to determine the rate of hydrolysis of the MAnh units when placed in water relative to the rate of reaction with aliphatic primary amines. Alternatively a complementary reactive group for the amine end-groups of PVP with better water stability than MAnh needs to be adopted.

Gels obtained in this study were used in two model studies discussed in Chapter 5.

References

(1) Pound, G.; McLeary, J. B.; McKenzie, J. M.; Lange, R. F. M.; Klumperman, B. *Macromolecules.***2006**, *39*, 7796.

(2) Pound, G.; Eksteen, Z.; Pfukwa, R.; McKenzie, J. M.; Lange, R. F. M.; Klumperman, B. *J. Polym. Sci. A.***2008**, *46*, 6575.

(3) Bathfield, M.; D'Agosto, F.; Spitz, R.; Charreyre, M.; Delair, T. *J. Am. Chem. Soc.* **2006**, *128*, 2546.

(4) Bathfield, M.; Daviot, D.; Agosto, F.; Spitz, R.; Ladaviere, C.; Charreyre, M.; Delair, T. *Macromolecules.***2008**, *41*, 8346.

(5) Yin, X.; Stover, H. D. H. *Macromolecules.***2002**, *35*, 10178.

(6) Qiu, X.-P.; Winnik, F. M. *Macromol. Rapid Commun.***2006**, *27*, 1648.

(7) Devine, D. M.; Higginbotham, C. L. *Eur. Polym. J.***2005**, *41*, 1272.

(8) Pavia; Lampman; Kriz *Introduction to spectroscopy third edition*; Brooks/Cole: Washington, **2001**.

(9) Ray, B.; Kotani, M.; Yamago, S. *Macromolecules.***2006**, *39*, 5259.

(10) Ranucci, E.; Ferruti, P.; Annunziata, R.; Gerges, I.; Spinelli, G. *Macromol. Biosci.* **2006**, *6*, 216.

(11) Liu, Z.; Rimmer, S. *Macromolecules.***2002**, *35*, 1200.

(12) Raith, K.; Kühn, A. V.; Rosche, F.; Wolf, R.; Neubert, R. H. H. *Pharm. Res.***2002**, *19*, 556.

(13) Luo, L.; Ranger, M.; Lessard, D. G.; Le Garrec, D.; Gori, S.; Leroux, J.-C.; Rimmer, S.; Smith, D. *Macromolecules.***2004**, *37*, 4008.

(14) Galgali, P.; Agashe, M.; Varma, A. J. *Carbohydr. Polym.***2007**, *67*, 576.

(15) Mishra, G.; McArthur, S. L. *Langmuir.***2010**, *26*, 9645.

(16) Qian, H.; Zhang, Y. X.; Huang, S. M.; Lin, Z. Y. *Appl. Surf. Sci.***2007**, *253*, 4659.

(17) Mishra, M. M.; Sand, A.; Mishra, D. K.; Yadav, M.; Behari, K. *Carbohydr. Polym.* **2010**, *82*, 424.

(18) Bueno, V.; Cuccovia, I.; Chaimovich, H.; Catalani, L. *Colloid Polym. Sci.***2009**, *287*, 705.

(19) Plunkett, K. N.; Kraft, M. L.; Yu, Q.; Moore, J. S. *Macromolecules.***2003**, *36*, 3960.

(20) Kim, J. S.; Park, J. S.; Kim, S. I. *React. Funct. Polym.***2003**, *55*, 53.

(21) Karadağ; Erdener; Saraydın; Dursun *Polym. Bull. (Berlin).***2002**, *48*, 299.

(22) Şahiner, N.; Saraydin, D.; Karadağ, E.; Güven, O. *Polym. Bull. (Berlin).***1998**, *41*, 371.

Chapter 5

5.1) Introduction

During the course of this study, two preliminary model studies regarding potential applications of the gels were conducted. The first model study investigated peptide-gel interaction/attachment. The second model study focussed on the potential toxic effects that the gels exhibit when placed in direct contact with rodent cardiac myoblast cells. Morphological changes that take place in cells that are placed in direct contact with the gels were monitored. These results were quantified by means of fluorescence microscopy.

5.1.1) Model study 1: *Peptide-gel attachment*

5.1.1.1) Requirements for biomaterials

Biomaterials are defined as synthetic materials, which have been designed to encourage a specific biological activity. Biomaterials can be placed inside the human/animal body without rendering damage to the surrounding tissue [1,2]

Biocompatibility refers to the coexistence of the implanted material and the surrounding tissue. A material is regarded as biocompatible if it can coexist in the host without any adverse reactions to the host body.[1,2] Alternatively "the ability of a material to perform with an appropriate host response in a specific application".[3,4] Biomaterials need to be biochemically compatible, non-toxic, non-irritable, non-allergenic, non-carcinogenic and biomechanically compatible with surrounding tissues. Last but not least, a bio-adhesive contact must be established between the living tissue and the materials. Different host systems will react differently to the material, so *e.g.* compatibility with the respiratory system does not necessarily mean that the material will be compatible with the digestive system. Biocompatibility has to be evaluated on a case by case basis.

When considering biocompatible systems, it is worth mentioning the physiological conditions found in the body. The temperature of the normal human body is around 37.4 °C. However, deviations over a temperature range of 33 – 42.5 °C have been reported. pH values vary over a wide

range of 1.0 (gastric content) to 7.4 (blood). Furthermore, pH values can change depending on health conditions.

5.1.1.2) Biocompatibility and molecular recognition

When designing biomaterials it is worth taking note of the interaction of a cell with a biomaterial established by the absorbed proteins. The cytoskeleton of the cell is typically made up of proteinaceous structures. These proteins can rearrange themselves when required, for example when the cell changes shape due to response to external stimuli. It is believed that protein adsorption is the first event that takes place when a cell comes into contact with a material. The adsorbed protein layer is then the cause for subsequent biological reactions.[5,6]

Living organisms make use of molecular recognition as a means to convey information. In diagnostics and drug delivery for example, it may be necessary to immobilize proteins onto polymers in order for the organisms to recognise these and not reject as foreign objects. The biological properties of the proteins need to remain intact, so the polymers are often attached to a site on the protein not required for molecular recognition.[7,8] Proteins are also regarded as the most valuable player in mediating polymer-cell interaction.[3] The insertion of biologically active signals onto the materials can be achieved by the chemical linkage of synthetic proteins and or peptides.[9]

The use of the binding motif arginine-glycine-aspartic acid (RGD) has been reported to have a stimulatory effect on cells in contact with this sequence.[9-11] Immobilization of RGD peptides has been a popular approach for modification of biomaterials. This sequence promotes cell adhesion via interaction with specific receptors in the plasma membrane.[12]

The first model study focused on a homo-polymer of one of the amino acids similar to those found in proteins, namely poly(benzyl-glutamate) (PBG).[13] This peptide is of particular interest as it is a homopolymer with the ability to form a helix.[14] PBG was synthesized (within the research group) and as a result served as an ideal model, as it serves as a mimic for the attachment of a polypeptide to MAnh in P(STY-*alt*-MAnh). Maleic anhydride containing copolymers are regarded as preactivated polymers as a result of the maleic anhydride moiety present in the polymer chains. As mentioned before, this moiety is highly susceptible to reactions with primary and secondary amines yielding amides and/or imides.[7]

5.1.2) Model study 2: *Cell viability studies*

5.1.2.1) In vitro tests

These experiments are performed in order to determine if the material is toxic when in contact with a particular cell line. Cytotoxicity tests are usually the primary method for the assessment of biocompatibility of a material.[15] Sterilization of the samples is carried out to ensure all other micro-organisms present on and in the sample are removed. The samples are incubated in the culture solution containing mammalian cells (direct contact) for 24 hours at 37.4 °C. The choice of cell types will depend on the desired application of a given biomaterial.[16] In general, fibroblast cells are used for primary assessment of cell adhesion. The reason for this is that these cells can easily proliferate on material surfaces. This model study focussed on the morphological changes and behaviour of the cells when placed in direct contact with the gels.

For more than 150 years, the morphological changes that occur in cells have been used to describe and identify cell death.[17] During the last few decades, characterization has been achieved on the molecular level. Morphological changes of the cells include shrinkage of cells, blebbing, and formation of apoptotic bodies. These can be observed by using optical light microscopy and serve as one of the earliest signs of cell death.[17,18] These results were confirmed by fluorescence microscopy.

5.2) Experimental details

5.2.1) Materials

Model study 1 - (Peptide-gel interaction/attachment): P(STY-*alt*-MAnh) ($M_{n(SEC)}$ = 35 000 g/mol, Đ = 4.6) and PBG ($M_{n(SEC)}$ = 7000 g/mol) were synthesized within the research group.

Model study 2 – (Cell viability):

Cell morphology: Claycomb medium (51800 C, Sigma-Aldrich) was supplemented with 10 % fetal bovine serum (12103 C, Batch 8A0177, SAFC Biosciences), 2 mM L-glutamine (G7513, Sigma-Aldrich), 0.1 mM norepinephrine [(±)arterenol] (A0937, Sigma-Aldrich) and penicillin-streptomycin (100 U/ml - 100 µg/ml) (P4333, Sigma-Aldrich). The HL-1 mouse cardiomyocyte cell line, were grown as a monolayer in a humidified atmosphere (95 % air, 5 % CO_2 at 37 °C). All growing surfaces were coated for 1 hour with a gelatin-fibronectin. 1 mL of Fibronectin (F-1141, Sigma-

Aldrich) was diluted in a 0.02 % Gelatin (G9391, Sigma-Aldrich) solution. Treatments were autoclaved at 120 °C to ensure sterility. The HL-1 mouse cardio myocyte cell line was established by Professor William C. Claycomb (Department of Biochemistry and Molecular Biology, LSU Health Sciences Centre, New Orleans, USA)[19] and donated by Delita Otto from the Cardio metabolic Research Group under supervision of Prof. F. Essop (Department of Physiological Studies, University of Stellenbosch)

Fluorescence microscopy: Rodant cardiac myoblast (H9c-2) cells were donated by Dr. Ben Loos of the Cell Death Group of the Department of Physiological Studies, University of Stellenbosch. All treatments were sterilized by UV-radiation to ensure treatments were sterile before being brought into contact with the cells. Propidium iodide (PI, Sigma, P4170) and Hoechst (Hoechst 33342, Sigma) dyes were used for fluorescence studies.

Note on the fluorescence dyes: Fluorescence microscopy is used to identify two types of cell death, namely apoptosis and necrotic cell death. Propidium Iodide (PI) is a membrane-impermeable dye which binds with the DNA. The uptake of this dye is therefore a sign for the loss of membrane integrity, indicating necrotic cell death. On the other hand, Hoechst fluorochrome is used to assess condensation of chromatin and/or cell shrinkage. This indicates nuclear condensation, which serves as a sign that apoptosis is taking place. Fluorescence studies provide detailed information regarding apoptotic and necrotic cell death, resulting in accurate information regarding cell viability and/or potential cytotoxicity effects.

5.2.2) Instrumentation

5.2.2.1) Light microscope

A CKX41 inverted microscope was used to check cell viability in the cell cultures. The microscope is fitted with a UIS2 (Universal Infinity corrected system) optic (x10 and x20 objectives). The light source was a 6 V/ 30 W halogen lamp, a lamp socket (U-LS30-3-2), built-in frosted and heat absorbing filters and a detachable illuminator.

5.2.2.2) Fluorescence microscope

Samples were observed on an Olympus Cell^{R} system attached to an IX-81 inverted fluorescence microscope equipped with an F-view-II cooled CCD camera (Soft Imaging Systems). Using a Xenon-Arc burner (Olympus Biosystems GMBH) as light source, images were excited with the 360 nm, 472 nm or 572 nm excitation filter. Emission was collected using a UBG triple- bandpass emission filter cube. Images were processed and background-subtracted using the Cell^{R} software.

5.2.3) Synthetic section

5.2.3.1) Model study 1*: Peptide-gel interaction*

5.2.3.1.1) Modification of P(STY-alt-MAnh)

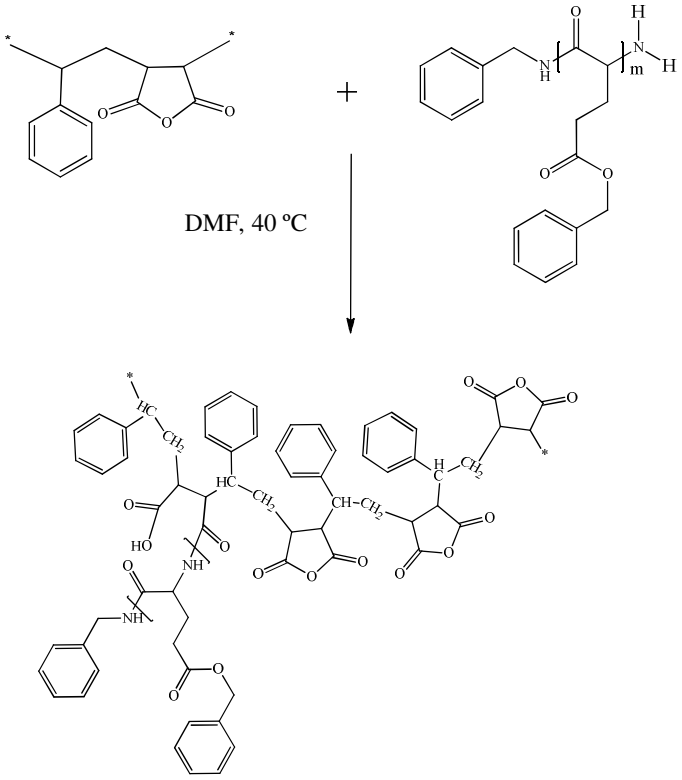

Scheme 5.1: Reaction between amine (end) functionalized PBG and P(STY-alt-MAnh).

PBG (0.116 g, 1.657x10^{-5} mol) and P(STY-*alt*-MAnh) (0.033 g, 1.657x10^{-4} mol MAnh) were dissolved in 120 µL reaction grade DMF. The reaction was left to proceed at 40 ºC for 12 hours. The

product was precipitated in diethyl ether and dried under vacuum for 6hours. ATR-FTIR spectroscopy was used for characterization. *Note: All calculations were based on moles of MAnh.*

5.2.3.1.2) Gel formation of P(STY-alt-MAnh)-g-PBG and PVP(NH$_2$)$_2$

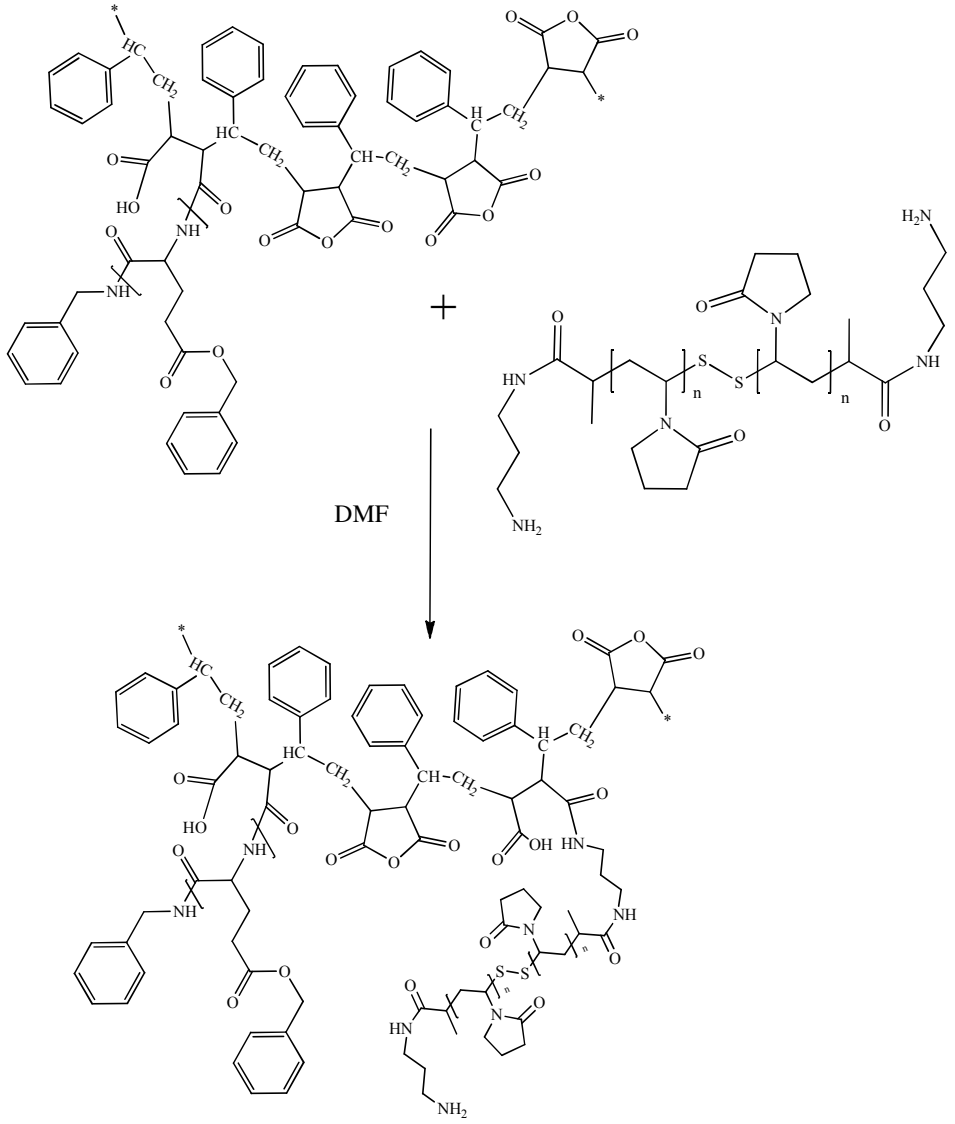

Scheme 5.2: Reaction between P(STY-alt-MAnh)-g-PBG and PVP(NH$_2$)$_2$.

PBG (0.116 g, 1.657x10^{-5} mol) and P(STY-*alt*-MAnh) (0.033 g, 1.657x10^{-4} mol MAnh) was dissolved in 120 µL reaction grade DMF. The reaction was left to proceed at 40 ºC for 12 hours. The product was precipitated in diethyl ether and dried under vacuum. PVP(NH$_2$)$_2$ ($M_{n(NMR)}$: 3000 g/mol, $M_{n(SEC)}$: 3000 g/mol, $Đ$ = 1.18) (0.447 g, 4.191x10^{-4} g/mol) was dissolved in 67 µL DMF. This solution was added to P(STY-*alt*-MAnh)-*g*-PBG. A gel formed over 24 hours.

5.2.3.2) Model study 2: *Cell viability*

5.2.3.2.1) Cell work procedure to monitor cell morphology

The supplemented cell medium was placed in gelatin-fibronectin coated 6-well plates (2 mL per well). Gels were rinsed with 70 % ethanol for sterility, and then rinsed with PBS, after which they were placed into the 6-well plates and allowed to equilibrate in the medium at 37 °C for an hour. The plates were removed from the incubator and the medium was refreshed with warm supplemented medium. Cells were then seeded ($1x10^5$ cells per well). The cells were incubated at 37 ˚C for 24 hours in the presence of the gels. Any signs of cell growth characteristics, movement of the cells and morphological changes of the cells were monitored with the light microscope.

Culturing and light microscopy of rodent cardiac myocyte (HL-1) cells were carried out by Delita Otto of the Cardio metabolic Research Group of the Department of Physiological Studies, Stellenbosch University. Images were acquired on a CKX41 light microscope (Olympus) with a 10x objective.[20]

5.2.3.2.2) Fluorescence microscopy study

H9c-2 rodent cardiac myoblast cells were seeded at a density of $1x10^5$ mL^{-1} into petri dishes, and grown to a confluency of 70-80 %. The gels were sterilized by means of UV radiation and placed incontact with the cells for 24 hours. Hoechst and PI, in a 1:200 dilution in PBS, were directly added onto the cells, using a final concentration of 50 µg/mL and 1 µg/mL respectively. Incubation time was 10 min and images were acquired immediately thereafter. Studies were performed in triplicate.

5.2.4) Results and discussion

5.2.4.1) Model study 1

PBG was reacted with P(STY-*alt*-MAnh), on the basis that the primary amine group present on the PBG will readily react with P(STY-*alt*-MAnh) via a simple ring-opening reaction. The mole ratio calculation for this reaction had to take into account that the majority of the MAnh units had to be available for the reaction with $PVP(NH_2)_2$. So in theory at least 90 % of the MAnh units had to remain intact for the reaction with $PVP(NH_2)_2$.

ATR-FTIR spectroscopy was used to characterize P(STY-*alt*-MAnh)-*g*-PBG (*Figure 5.1*). The peak of interest was the -C=O of the P(STY-*alt*-MAnh) at 1838 cm^{-1} and 1774 cm^{-1},which was expected to shift to lower wave numbers when reacted with the terminal amine of PBG. The bottom spectrum in *Figure 5.1* shows the presence of both PBG and P(STY-*alt*-MAnh). In addition, *Figure 5.2* shows an enlargement of the area between 1500 – 2000 cm^{-1}, which clearly shows the carbonyl shift in the final product.

5.2.4.1.1) Modification of P(STY-alt-MAnh) with PBG:

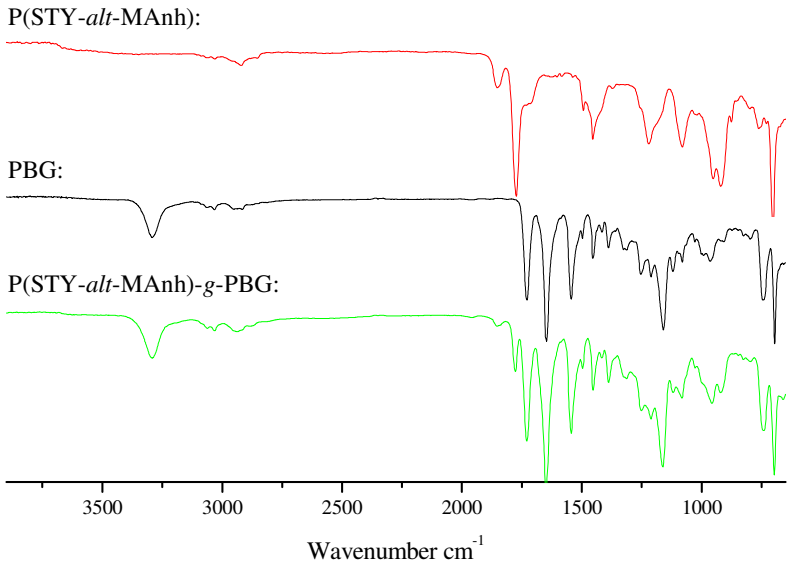

Figure 5.1: ATR-FTIR of P(STY-alt-MAnh)PBG.
Top spectrum: P(STY-alt-MAnh), Middle spectrum: PBG, Bottom spectrum: P(STY-alt-MAnh-g-PBG.

The mole ratio of PBG-NH_2: MAnh was 1: 10, and as a result, the majority of the MAnh remained unreacted. This caused a lot of difficulty when trying to observe the peaks of interest on the ATR-FTIR spectra, as the unreacted MAnh units masked those that reacted with PBG. In *Figure 5.2* a slight shift of the carbonyl peak is observed in the bottom spectrum. As in the case of the other gels, the amide peak formation is masked, in this case by the PBG peaks.

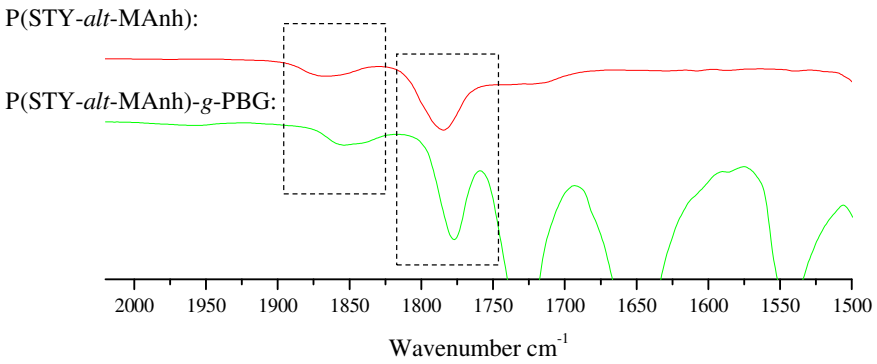

Figure 5.2: Enlargement of Figure 5.1 between 1500 – 2000 cm^{-1}.
Top spectrum: P(STY-alt-MAnh), Bottom spectrum: P(STY-alt-MAnh)-g-PBG.

The fact that there was only one amine group present on the high molecular weight PBG presented much difficulty. Reaction times were varied from 4 hours, to 6 hours, to 12 hours, to 24 hours and lastly to 72 hours. However, reaction time seemed to have had no influence on the reaction. From ATR-FTIR spectroscopy it was evident that both these polymers were present. There was no spectroscopic evidence of amide formation, which would be expected if the PBG did react with the MAnh on the P(STY-*alt*-MAnh). It is believed that this peak was masked by the (amide) peaks of PBG.

5.2.4.1.2) Gel formation of P(STY-alt-MAnh)-g-PBG and PVP(NH$_2$)$_2$

PVP(NH$_2$)$_2$ is a necessity in the gel as the swelling ratio is greatly dependent on the ratio of PVP(NH$_2$)$_2$ to P(STY-*alt*-MAnh) present in the gel sample. If the majority of the sample consisted of P(STY-*alt*-MAnh) and PBG, then swelling of the gel would be little to none, seen that these polymers are both hydrophobic. After addition of PVP(NH$_2$)$_2$, from ATR-FTIR spectroscopy it was apparent that bonding did indeed take place as expected. Shown in *Figure 5.3* are spectra for P(STY-*alt*-MAnh)-*g*-PBG–PVP(NH$_2$)$_2$gel and P(STY-*alt*-MAnh)-*g*-PBG. The overlap of peaks made characterization and assignment very difficult. From the spectra it was clear that the asymmetrical and symmetrical stretch of the –C=O was no longer present at 1838 cm^{-1} and 1774 cm^{-1}. Absorbance was expected at 1723cm^{-1}and 1680 cm^{-1} as a result of –COOH symmetrical stretch and the amide respectively. However, these are not visible due to the peaks of PVP(NH$_2$)$_2$ and PBG present at 1556 – 1700 cm^{-1}.[21]

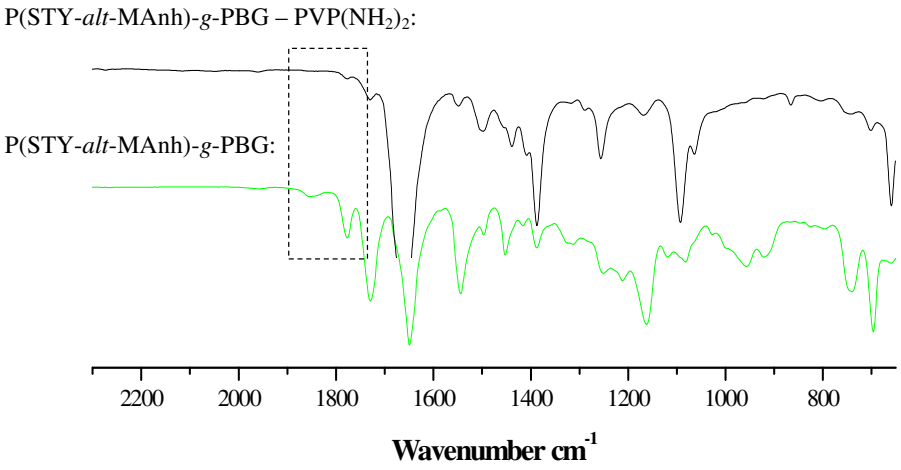

Figure 5.3: ATR-FTIR spectra of P(STY-alt-MAnh)-g-PBG– PVP(NH$_2$)$_2$ gel.
Bottom spectrum: P(STY-alt-MAnh)-g-PBG, Top spectrum: P(STY-alt-MAnh)-g-PBG–PVP(NH$_2$)$_2$ gel.

5.2.4.2) Model study 2

5.2.4.2.1) Cell viability

The second model study was to investigate the toxicity of the gels. As mentioned earlier, one of the first signs of unhealthy cells/poisoned cells would be the change in cell morphology.

In *Figure 5.4,* the negative control can be seen, the morphology of healthy cells, which have not been in contact with the gels. *Figure 5.5* shows the morphology of the cells after having been in contact with the gels for 24 hours.

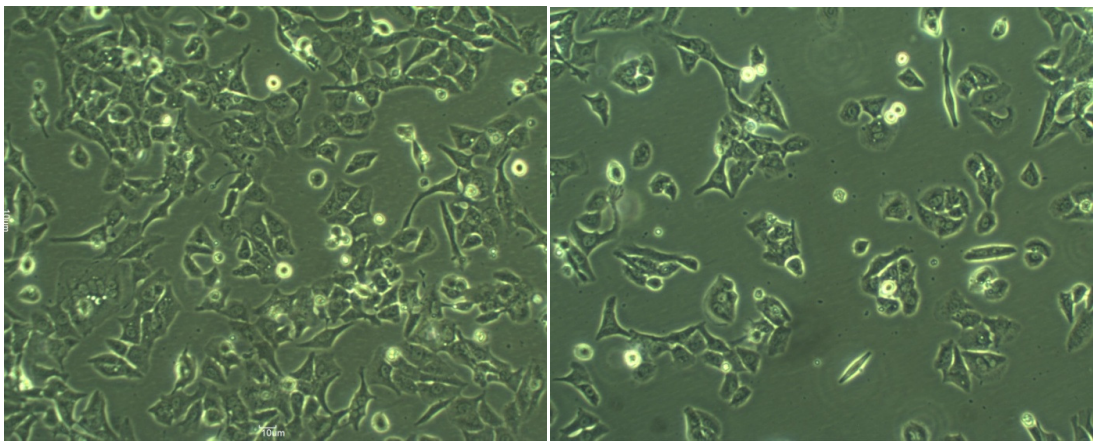

Figure 5.4: Negative cell control.
Cells that have not been in contact with the gels are shown here.
Photograph taken at different areas in the same cell well.

There is no indication of a decrease in growth density, or any morphological changes. The cells seem to be healthy and replicating at a reasonable rate despite the presence of the hydrogels. The cells seem to proliferate into a monolayer, which can be compared to the monolayer observed for the untreated cells in *Figure 5.4*. It was not possible to make a distinction between the control cells and the cells in the presence of the gels.

The general observation that was made is that the cells do not seem to be disturbed by the presence of the gels (*Figure 5.6*), and in most of the cases it was observed that the cells even migrated towards the gels. These studies were only qualitative and Fluorescence microscopy was used to quantify these results.

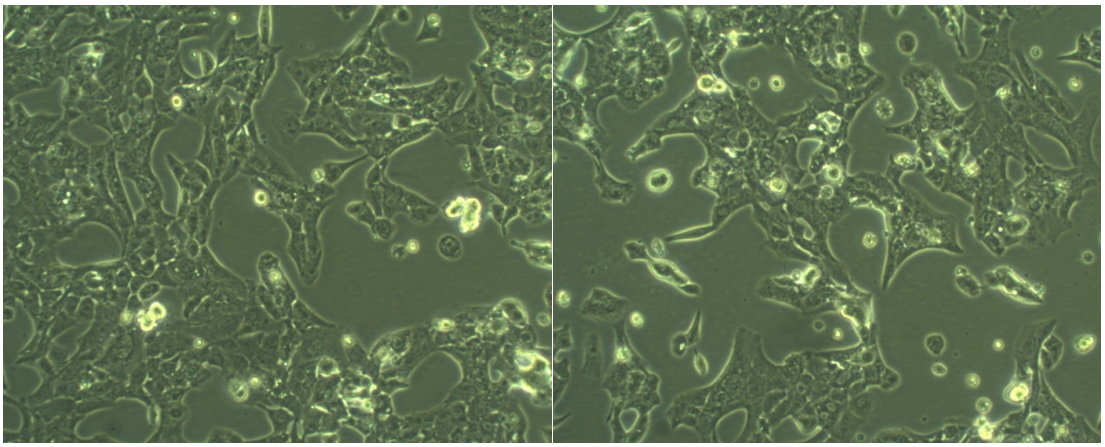

Figure 5.5: Cells in the presence of the gel.
Cells that have been incubated with the gels for 24hours are shown.
Photograph taken at different areas in the same cell well.

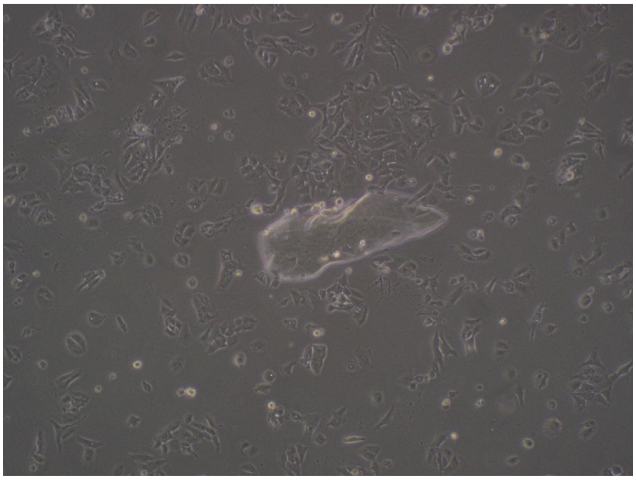

Figure 5.6: Cells surrounding the hydrogel after 24 hours.

5.2.4.2.2) Fluorescence microscopy

Fluorescence microscopy was used as an alternative method to investigate if the gels exhibit a toxic effect on the cells. The red dye (PI) only stains the nucleus if the cell has lost membrane integrity due to toxic effects or other causes resulting in loss of membrane integrity. The blue dye (Hoescht) stains the DNA and is used to assess the morphology of the nucleus of the cells. The negative control cells are shown in *Figure 5.7* and the positive control cells in *Figure 5.8*.

In *Figure 5.7 A*, the morphology of the healthy nuclei are seen, and *Figure 5.7 B* illustrates non-specific background signal. *Figure 5.7 C*, is an overlay of the blue and red channels. This will illustrate any loss of cell wall integrity in the case where cells experience toxic effects. If there is loss of cell wall integrity, the red dye would permeate through the cell wall and stain the nucleus red. *Figure 5.7 D*, shows the morphology of healthy cells and *Figure 5.7 E* is an overlay of red, blue and transmission in order to amplify contrast.

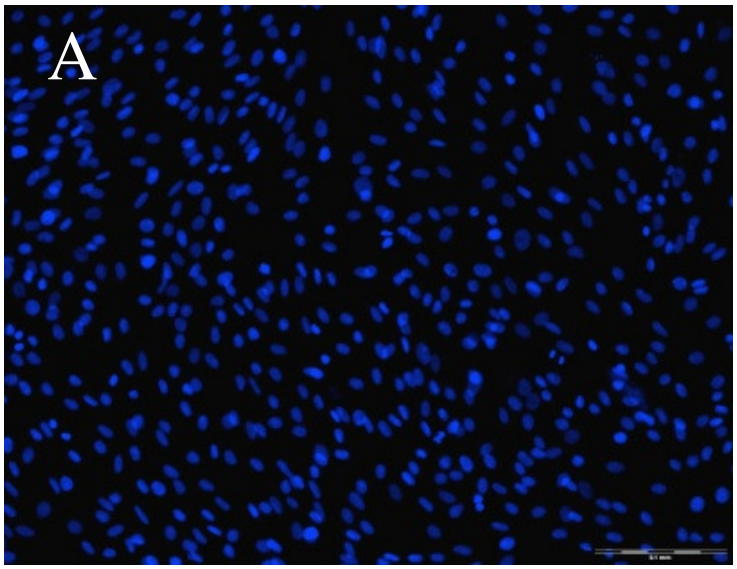

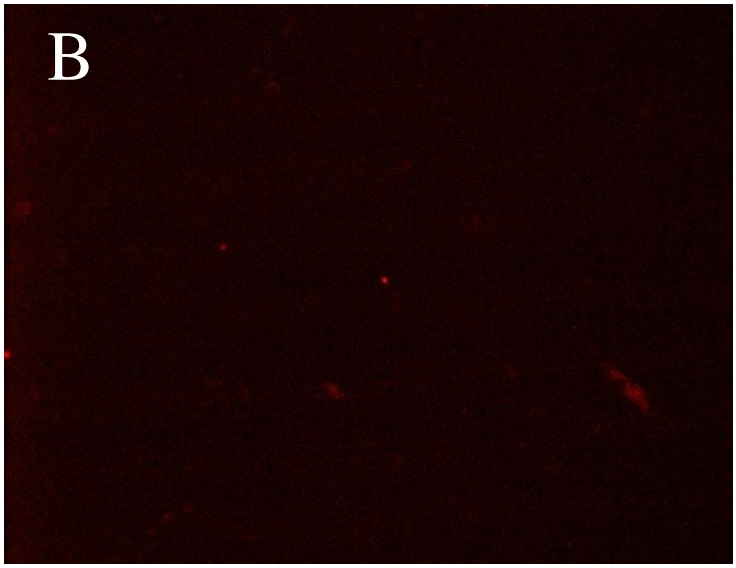

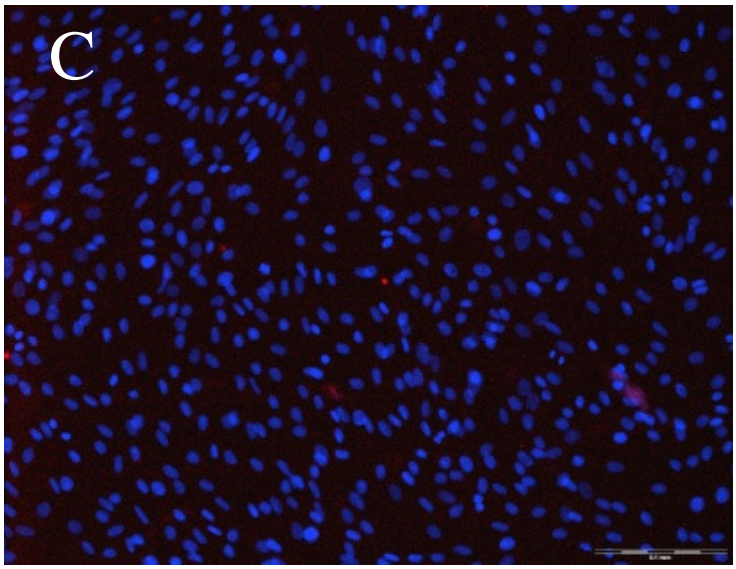

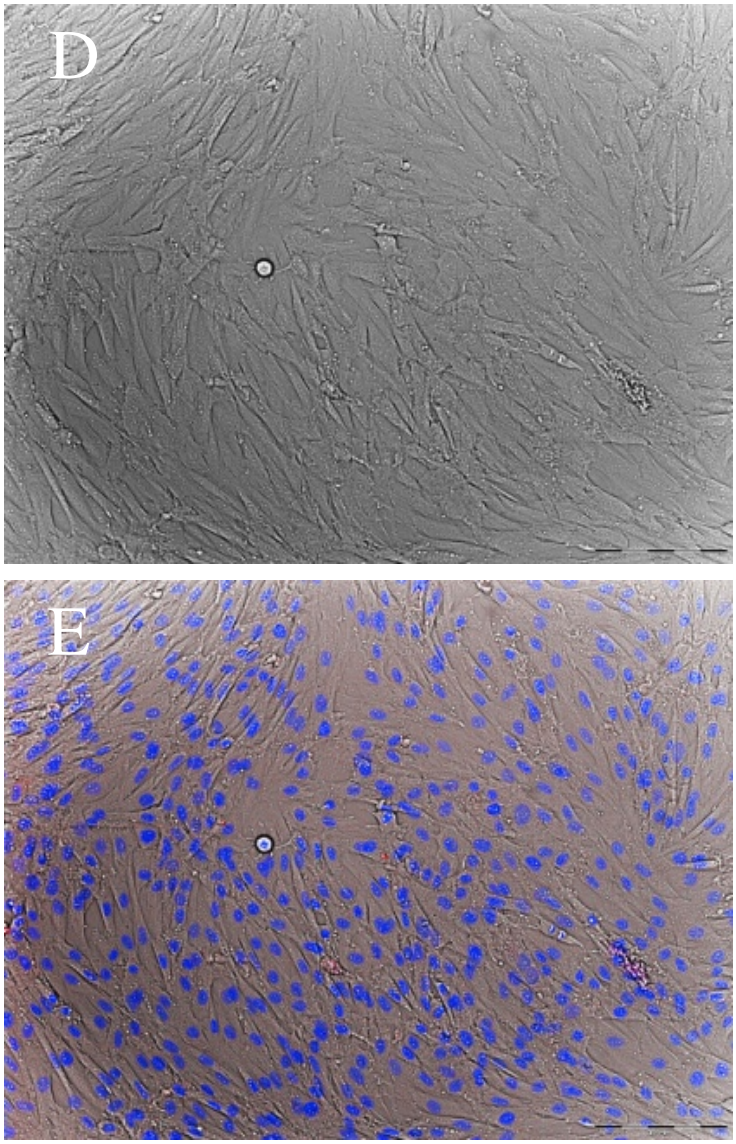

Figure5.7: Fluorescence images of negative control cells.
(A) Morphology of the nuclei. (B) Non-specific background signal. (C) Overlay of blue and red channels. (D) Morphology of the cells. (E) Overlay of blue, red and transmission channels.

In *Figure 5.8 A*, the morphology of the nuclei are seen. *Figure 5.8 B* illustrates nectrotic cell death. *Figure 5.8 C*, is an overlay of the blue and red channels, indicating apoptotic and nectrotic cell death. This illustrates loss of cell wall integrity, as the red dye permeated through the cell wall and stained the nucleus red. *Figure 5.8 D*, an overlay of red, blue and transmission in order to amplify contrast.

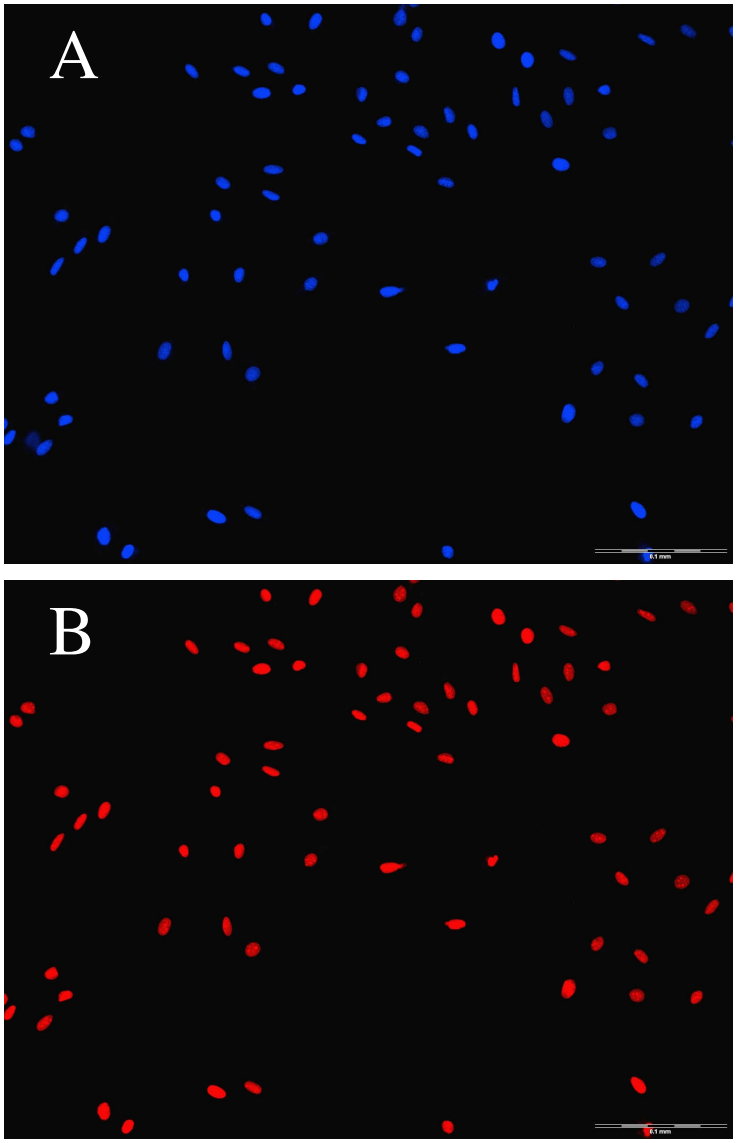

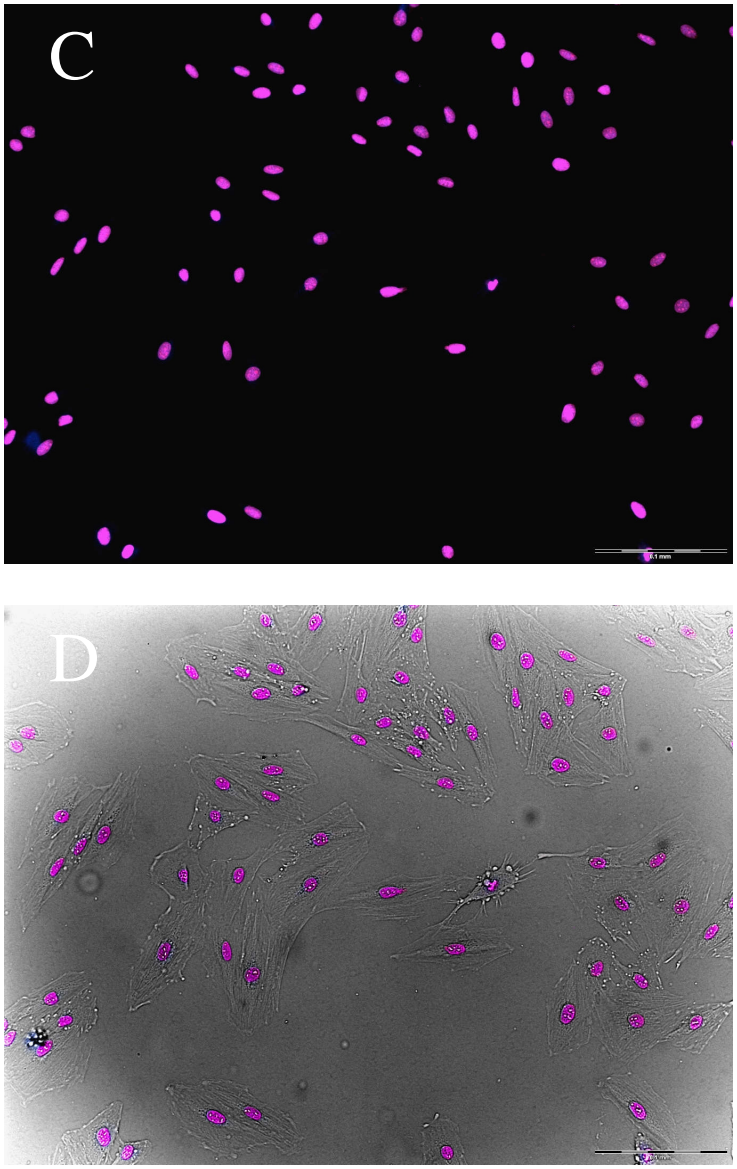

Figure 5.8: Fluorescence images of positive control cells.
(A) Morphology of the nuclei. (B) Indication of necrotic cell death (C) Overlay of blue and red channels. (D) Overlay of blue, red and transmission channels.

After the negative and positive cell controls were obtained, the gels were incubated with the cells as described previously. In *Figure 5.9* cells in contact with the gels are shown.

In *Figure 5.9 A*, the morphology of the healthy nuclei are seen. *Figure 5.9 B* illustrates non-specific interaction of the dye with the gels. *Figure 5.9 C*, is an overlay of the blue and red channels, indicating no apoptotic and/or nectrotic cell death. When a cell experiences undesirable conditions, often the nuclei condense, and with fluorescence microscopy it is seen as brighter nuclei compared to the rest. In *Figure 5.9 C*, nuclei that could have possibly undergone condensation as a result of toxic

effects appear brighter, although an alternative explanation would be that these cells are simply busy dividing and would also appear brighter. However, the morphology of the nuclei (*Figure 5.8 A*) and the morphology of the cells (*Figure 5.8 D*) do not show any signs of cells being in distress. Both of these morphologies compare very well to the control cells. Furthermore, compared to the hundreds of healthy cells in the same environment, the nuclei that possibly experienced a minor toxic effect, are not of any statistical significance.

Figure 5.9 D, shows the morphology of the cells, and when compared to the negative control, no distinctions can be made. *Figure 5.9 E,* shows an overlay of red, blue and transmission in order to amplify contrast.

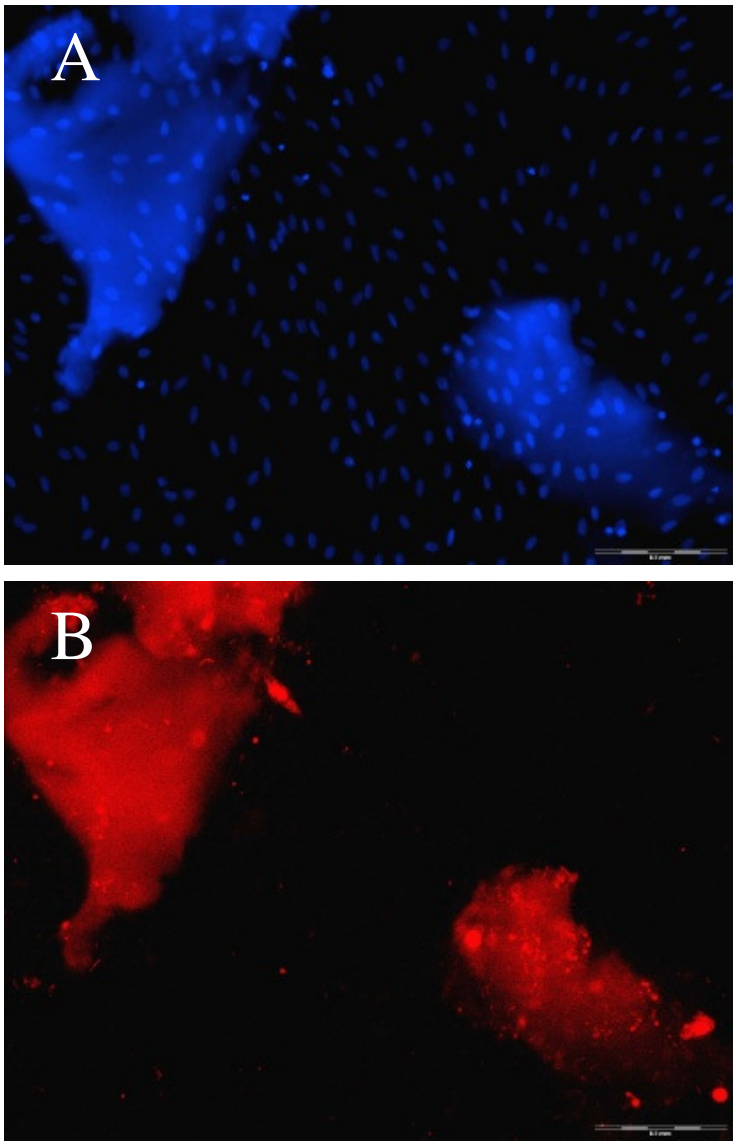

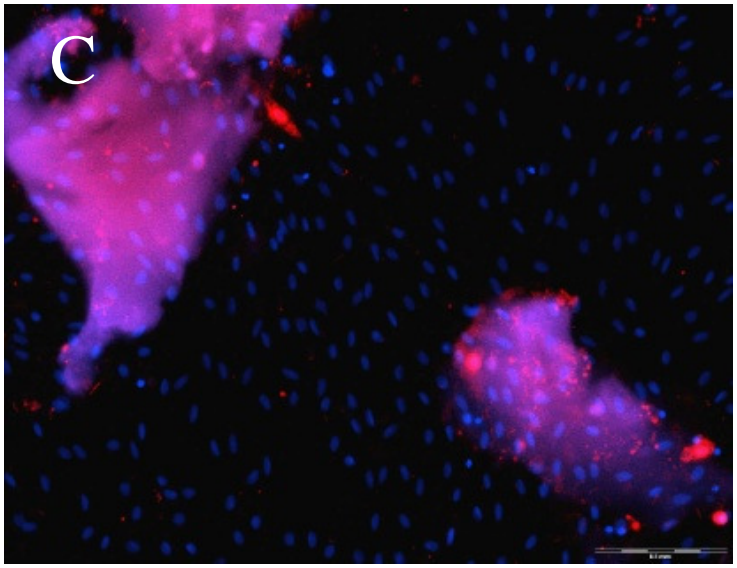

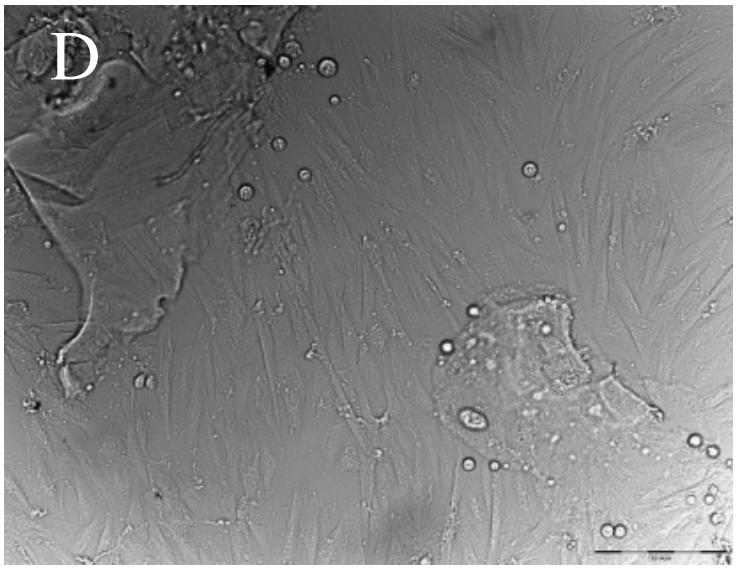

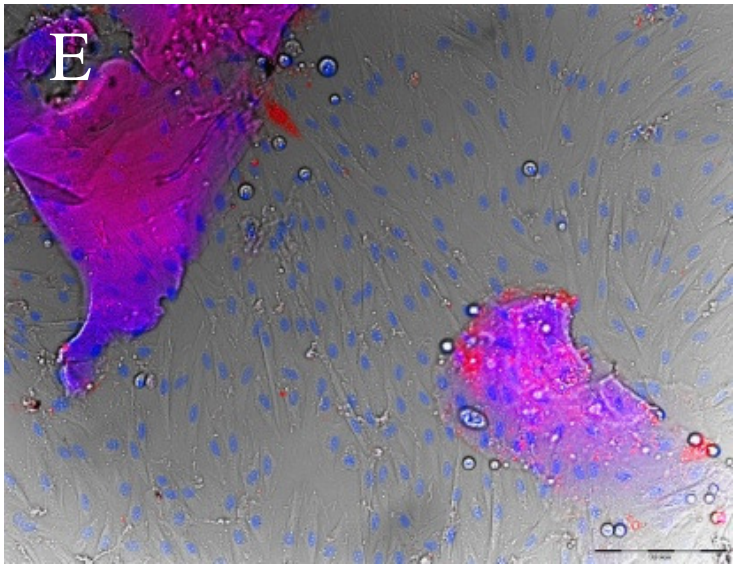

Figure 5.9: Fluorescence images of cells in contact with gels for 24hours.
(A) Morphology of the nuclei. (B) Non-specific background signal. (C) Overlay of blue and red channels. (D) Morphology of the cells. (E) Overlay of blue, red and transmission channels.

5.3) Conclusion

Model study 1: The aim of this study was to lay ground work in order to optimize reaction conditions so that PBG (representative of a synthetic peptide[13,14]) can be replaced by a peptide containing the RGD sequence that would enhance molecular recognition, stability of the material in the cell environment and cell adhesion onto the materials.[8,22-26] This would in turn open another wide field in the research of biocompatible materials.[27-31] Characterization proved to be challenging, however just because characterization was not entirely possible by means of ATR-FTIR spectroscopy, it does not mean that the reaction did not take place. In order to confirm the attachment of PBG to P(STY-*alt*-MAnh) additional work will have to be performed with High Pressure Liquid Chromatography.

Model study 2: Although very little morphological cell changes were observed after 24 hours, it would be advised to do more experiments. For example, the MTT assay could be used to determine the percentage of metabolically viable cells after exposure to the gels.[20]

It can be concluded that the cells did not undergo adverse side reactions in the presence of the gels as fluorescence microscopy did not indicate cell death, however it would be advisable to vary the incubation times and amounts of the gel placed in contact with the cells.

References

(1) Liu, Y.; Li, J. P.; Hunziker, E. B.; de Groot, K. *Phil. Trans. R. Soc. A.***2005**, *364*, 233.

(2) Beyermann, M.; Bienert, M.; Niedrich, H.; Carpino, L. A.; Sadat-Aalaee, D. *J. Org. Chem.***1990**, *55*, 721.

(3) Chen, H.; Yuan, L.; Song, W.; Wu, Z.; Li, D. *Prog. Polym. Sci.***2008**, *33*, 1059.

(4) Ratner Buddy, D.; Hoffman Allan, S. In *Hydrogels for Medical and Related Applications*; American Chemical Society: **1976**; Vol. 31, p 1.

(5) Ratner, B. D.; Bryant, S. J. *Annu. Rev. Biomed. Eng.***2004**, *6*, 41.

(6) Anderson, J. M. *Annu. Rev. Mater. Res.***2001**, *31*, 81.

(7) Ladaviere, C.; Delair, T.; Domard, A.; Novelli-Rousseau, A.; Mandrand, B.; Mallet, F. *Bioconjugate Chem.***1998**, *9*, 655.

(8) Jin Yoon, J.; Ho Song, S.; Sung Lee, D.; Park, T. G. T. G. *Biomaterials.***2004**, *25*, 5613.

(9) Furth, M. E.; Atala, A.; Van Dyke, M. E. *Biomaterials.***2007**, *28*, 5068.

(10) Sasai, Y.; Kondo, S.; Yamauchi, Y.; Kuzuya, M. *J. Photopolym. Sci. Technol.***2009**, *22*, 503.

(11) Sasai, Y.; Kondo, S.; Yamauchi, Y.; Kuzuya, M. *J. Photopolym. Sci. Technol.***2010**, *23*, 595.

(12) Zhang, Z.; Lai, Y.; Yu, L.; Ding, J. *Biomaterials.***2010**, *31*, 7873.

(13) Baier, R. E.; Zisman, W. A. *Macromolecules.***1970**, *3*, 70.

(14) Doty, P.; Bradbury, J. H.; Holtzer, A. M. *J. Am. Chem. Soc.***1956**, *78*, 947.

(15) Rogero, S. O.; Malmonge, S. M.; Lugão, A. B.; Ikeda, T. I.; Miyamaru, L.; Cruz, Á. S. *Artif. Organs.***2003**, *27*, 424.

(16) Devine, D. M.; Devery, S. M.; Lyons, J. G.; Geever, L. M.; Kennedy, J. E.; Higginbotham, C. L. *Int. J. Pharm.***2006**, *326*, 50.

(17) Ziegler, U.; Groscurth, P. *Physiology.***2004**, *19*, 124.

(18) Smith, L. E.; Rimmer, S.; MacNeil, S. *Biomaterials.***2006**, *27*, 2806.

(19) Claycomb, W. C.; Lanson, N. A.; Stallworth, B. S.; Egeland, D. B.; Delcarpio, J. B.; Bahinski, A.; Izzo, N. J. *P.N.A.S.***1998**, *95*, 2979.

(20) Kirf, D.; Higginbotham, C. L.; Rowan, N. J.; Devery, S. M. *Biomed. Mater. (Bristol, U. K.).***2009**, *5*, 35002.

(21) Mishra, G.; McArthur, S. L. *Langmuir.***2010**, *26*, 9645.

(22) Zhang, D.; Duan, J.; Wang, D.; Ge, S. *Journal of Bionic Engineering.***2010**, *7*, 235.

(23) Lutz, J.-F.; Börner, H. G. *Prog. Polym. Sci.***2008**, *33*, 1.

(24) Luo, Y.; Wang, Y.; Niu, X.; Shang, J. *Eur. Polym. J.***2008**, *44*, 1390.

(25) Shakya, A. K.; Sami, H.; Srivastava, A.; Kumar, A. *Prog. Polym. Sci.***2010**, *35*, 459.

(26) Deng, C.; Chen, X.; Sun, J.; Lu, T.; Wang, W.; Jing, X. *J. Polym. Sci., Part A: Polym. Chem.***2007**, *45*, 3218.

(27) Jagur-Grodzinski, J. *Reactive and Functional Polymers.***1999**, *39*, 99.

(28) Chaterji, S.; Kwon, I. K.; Park, K. *Prog. Polym. Sci.***2007**, *32*, 1083.

(29) Drotleff, S.; Lungwitz, U.; Breunig, M.; Dennis, A.; Blunk, T.; Tessmar, J.; Göpferich, A. *Eur. J. Pharm. Biopharm.***2004**, *58*, 385.

(30) Thornton, P. D.; Mart, R. J.; Webb, S. J.; Ulijn, R. V. *Soft Matter.***2008**, *4*, 821.

(31) van Hest, J. C. M.; Tirrell, D. A. *Chem. Commun.***2001**, 1897.

Chapter 6

During the course of this study xanthate chain transfer agents were synthesized and characterized by means of ^{13}C and ^{1}HNMR spectroscopy. These were then used in the polymerization of NVP. This rendered PVP with narrow molar mass distributions, consisting of succinimide and xanthate functionalities at the α- and ω-chain ends respectively. The molar mass distribution of PVP-succinimide was determined and confirmed by means of ^{1}HNMR spectroscopy, SEC and MALDI-TOF-MS. The presence and removal of the respective functional groups was successfully confirmed by ^{1}H NMR, ATR-FTIR and UV-vis spectroscopy's.

PVP-succinimide was then modified by means of an aminolysis reaction with an excess of aliphatic diamine to render telechelic amino-functionalized PVP with narrow molar mass distribution to be used for the synthesis of gels. The post polymerization modification reaction was straightforward and reproducible, resulting in high purity polymers. The M_n of $PVP(NH_2)_2$ was determined via SEC and MALDI-ToF-MS. The expected M_n of the $PVP(NH_2)_2$ was that of two chains linked through a disulphide bond, being double that of the M_n of the unmodified polymer chain. Due to possible interaction of the polymer chain ends with the SEC column some broadening of the elution peaks occurred (slightly higher dispersities than the unmodified polymer). The successful removal of the succinimide and xanthate functionalities after aminolysis was confirmed by means of ^{1}H NMR, ATR-FTIR and UV-vis spectroscopy's.

Telechelic amino-functionalized PVP was cross-linked with P(STY-*alt*-MAnh) to form a polymeric gel network. The successful gel formation served as further proof that the $PVP(NH_2)_2$ was indeed telechelic amino-functionalized. The gels were stable in aqueous media and had an equilibrium water content between 60 % – 750 %, which depended on PVP/P(STY-*alt*-MAnh) ratio and on molar mass of the PVP. These results indicated that the water content of these hydrogels were indeed suitable for biological applications.[1,2]

The use of DMF for the synthesis of the gels was a major cause of concern with regards to toxicity. Modification of P(STY-*alt*-MAnh) was achieved by attachment of PEG onto the styrene moiety. This resulted in P[(PEG-STY)-*alt*-MAnh] that was readily soluble in water. However, gelation time was not desirable and for toxicity studies, focus of this study was shifted to $PVP(NH_2)_2$ and P(STY-*alt*-MAnh) gels.

Chapter 6
Conclusion

Two model studies were performed on the gels. In the first model study, the attachment of a synthetic peptide, PBG, onto P(STY-*alt*-MAnh) was successful and also resulted in successful gel formation. In terms of characterization, with ATR-FTIR spectroscopy it was difficult to quantify the attachment as a result of the low percentage of MAnh that was allowed to react. The majority of the MAnh remained intact and masked the signals of the reacted units. However a slight shift of the -C=O stretch of the MAnh in the ATR-FTIR spectrum was observed. After reaction with $PVP(NH_2)_2$, attachment was confirmed by means of ATR-FTIR spectroscopy, as the -C=O peak was no longer visible.

In the second model study, from monitoring the morphological changes of the cells placed in direct contact with the gels, it was concluded that the cells had no adverse reaction to the presence of the gels. If the gels were toxic there would not have been any live cells observed after 24 hours. With the use of fluorescence microscopy, the identification of the live and dead cells after contact with the gels was quantified. Although a limited number of changes in the nuclei were observed, the toxic effects were minor when compared to the hundreds of healthy living cells present after being in contact with the gels.

References:

(1) Şahiner, N.; Saraydin, D.; Karadağ, E.; Güven, O. *Polym. Bull. (Berlin)***1998**, *41*, 371.

(2) Karadağ, E.; Dursun, S. *Polym. Bull. (Berlin)***2002**, *48*, 299.